Journal of Building Engineering 91 (2024) 109719

Contents lists available at ScienceDirect

Journal of Building Engineering

journal homepage: www.elsevier.com/locate/jobe

A comprehensive review on fresh and rheological properties of 3D printable cementitious composites

Mahfuzur Rahman [a], S. Rawat [a], Richard (Chunhui) Yang (Chunhui)[a], Ahmed Mahil [b], Y.X. Zhang [a,*]

[a] Centre for Advanced Manufacturing Technologies, School of Engineering, Design and Built Environment, Western Sydney University, Penrith, NSW, 2751, Australia
[b] Luyten, Melbourne, VIC, 3001, Australia

ARTICLE INFO

Keywords:
3D printing
Cementitious composites
Fibre reinforced cementitious composites
Fresh properties
Rheology

ABSTRACT

The undeniable potential of 3D printing technology to revolutionize global manufacturing processes has led to the emergence of advanced, digitalized, and fully automated construction techniques. Despite the growing interest in this technology, a significant challenge still exists in the development of cement-based printing material due to the complex interaction of various fresh and rheological property parameters. This review comprehensively explores fundamental fresh properties (flowability, buildability, extrudability, pumpability and open time) and rheological properties (static yield stress, dynamic yield stress, plastic viscosity) essential for the formulation of 3D printable cementitious composites, with and without fibres. The results obtained from different rheometers for successful 3D printed mixes are also summarized, highlighting variation in recorded values. Moreover, the review thoroughly investigates factors affecting both fresh and rheological properties, such as the type of supplementary cementitious materials, fibre type and dosage, superplasticizer, and viscosity-modifying admixture. It also identifies the clear impact of these parameters and further recommends the optimal range of some properties, such as a flowability value between 160 and 200 mm, to achieve desirable 3D printability of cementitious composites. Overall, this review offers valuable insights for developing new mix compositions suitable for 3D printing and serves as a useful tool in establishing guidelines for 3D printable cementitious composite materials, which are currently lacking but crucial for research, development, and application in this field.

1. Introduction

Additive manufacturing and 3D printing are commonly used interchangeably to describe computer-guided techniques for creating objects from electronic data sources. Today, 3D printing is considered a revolutionary technology, often referred to as *the fourth industrial revolution* [1,2], with its potential to dramatically transform global manufacturing processes. Among its revolutionary applications, 3D printing of cementitious composites (3DP-CC) take centre stage as a cutting-edge digital construction technique. As this technology evolves, it emerges as a promising pathway toward fully automating construction processes in the near future. In the process of 3D printing with cementitious composites, the material is pumped and extruded through a nozzle, accurately deposited in successive layers to create a three-dimensional object. The extruded material should be capable of supporting its own weight and

* Corresponding author.
E-mail address: sarah.zhang@westernsydney.edu.au (Y.X. Zhang).

https://doi.org/10.1016/j.jobe.2024.109719
Received 17 February 2024; Received in revised form 30 April 2024; Accepted 22 May 2024
Available online 23 May 2024

maintaining its shape without the need for formwork, while also bonding strongly with the adjacent layer. Compared to conventional concrete manufacturing techniques, 3DP-CC represents an innovative, automated, digital approach with multiple advantages. This technology eliminates the need for formwork, which typically constitutes 50 % of total construction costs [3] and consumes up to 70 % of construction time [4]. Additionally, 3DP-CC contributes to cost reduction through efficient waste disposal practices by utilizing recycled construction materials as mix constituents, enhancing sustainability. Booya et al. [5] suggested that employing 3D printing in construction can potentially reduce labour costs by 50–80 % and decrease construction waste generation by 30–60 % compared to traditional methods. Notably, 3DP-CC can fabricate intricate structures within hours [6–8], a feat challenging for conventional formwork-dependent casting techniques. Additionally, it enhances construction safety by reducing the occurrence of on-site accidents while also gaining recognition for its eco-friendly attributes [9]. The distinct goals and indicators influenced by this technology include the adoption of advanced construction technologies, which would lead to a reduction in carbon emissions, the provision of secure and affordable housing, and the efficient use of natural resources [10].

Although 3DP-CC is a new and emerging technology, several 3D printed structures have already been constructed. The history of 3D printing dates back to 1939 when William E. Urschel created the first 3D printed concrete building [11]. In 2004, Enrico Dini developed a D-shaped 3D printer for large structures using sand and binders. Winsun, a Chinese construction firm, used a massive 3D printer to create cost-effective houses and built a 5 stored residential building in 2014 [12]. 3DP-CC is also a promising technique for constructing structural space habitats on the moon and Mars, as well as for military purposes. Companies like ICON, USA and NASA are working together on projects such as Olympus and Mars Dune Alpha to create structures on the Moon and Mars using 3DP-CC [13]. The European Space Agency also initiated a program in 2009 to use 3DP-CC to build safe habitats on the Moon [14]. 3DP-CC has also been used to produce prefabricated structural elements and printed furniture. Some other structures already constructed with 3DP-CC technology includes Lotus house in China, three-story DFAB house in Switzerland [15], and arches for vehicle hiding in California [16].

Despite these advancements, the widespread adoption of 3DP-CC faces a key challenge mainly due to the intricacies involved in the development of a suitable printing material. When designing 3D printable mix, it is crucial to consider fresh property parameters such as flowability, buildability, extrudability, pumpability and open time [17]. These parameters differ significantly from those considered in conventional mould-cast mixes. Unlike traditional methods that rely on formwork, 3D printable mixes must be strong enough to support their own load layer by layer without causing deformation, and simultaneously, must be flowable enough to move through pipes during the printing process. These requirements go beyond the concrete specifications outlined in international standards [17, 18]. To enhance the understanding in this area, several review studies have been published recently on different aspects of the research and development on 3DP-CC as summarized in Table 1.

It can be observed from Table 1 that the existing reviews on 3DP-CC primarily delve into mix design concepts [18,22], sustainability concerns [10,19,26], durability aspects [23], reinforcement strategies [22,24,27], fresh and hardened material properties of 3D printed concrete [4,23,25] and effects of fibre inclusion on 3DP-fibre reinforced cementitious composite (3DP-FRCC) [20,21]. However, there remains a lack of a clear understanding of the fundamental fresh and rheological properties that are most crucial for

Table 1
Main focuses of the latest review papers on 3DP-CC.

Category	Main focuses	Publication Year	Reference
Material Development and Process Parameters for 3D Printing	Raw material properties, mechanical properties, reinforcement strategies, applications of 3D printing and sustainability concerns	2023	[4]
	Different process parameters associated with 3D printing, monitoring and diagnosis in 3D printing with sustainability concerns	2023	[19]
	Effects of fibre inclusion on the printability properties, interlayer adhesion and anisotropic effects on mechanical properties	2023	[20]
	Effects of fibres on fresh and hardened properties for cement and geopolymer based composites	2023	[21]
	Material characteristics for 3D printing, mix designs, reinforcement strategies for large scale 3D printing construction	2022	[22]
	Fresh and hardened property assessment methods, different durability performance aspects for different types of 3DP-CC.	2022	[23]
	Different mix design methods, material properties, mechanical and durability aspects in 3D printed concrete.	2021	[18]
	Fresh concrete behaviour during and after 3D printing, reinforcement methods, shrinkage, and sustainability concerns.	2021	[24]
	Overall printing process and phases, mechanical properties as well as durability aspects focusing particularly on 3DP-ECC	2020	[25]
Sustainability Aspect	Different sustainable materials employed for 3D printing as well its growth analysis in building sector and different technical methods employed for 3D printing, pros, and challenges	2023	[26]
	Recycled materials used for 3D printing as well as different printing parameters effect and reinforcement methods, cost, and environmental impact analysis	2023	[27]
	Sustainability aspects of binders used for 3D printing aspect, alternative cementitious materials	2021	[10]
Rheological Aspect	The pumpability property of 3D printable concrete and the corresponding rheological properties	2023	[28]
	Detailed thixotropic structural build up evaluation in 3D printing	2021	[29]

formulating novel 3D printable mixes. While some review papers briefly touch on these parameters, there is a lack of detailed analysis of critical aspects such as in-depth investigations into test procedures adopted for assessing fresh property parameters, factors influencing both fresh and rheological properties, and diverse rheological test outcomes for different 3D printable mixes as depicted in Fig. 1.

This review paper presents an in-depth investigation of all the parameters mentioned in Fig. 1 and provides a comprehensive summary of various testing procedures and results related to fresh and rheological properties. The paper further provides a thorough understanding of the factors influencing these properties, such as type of supplementary cementitious material (SCM), fibre type and dosage, chemical admixture such as superplasticizer (SP) or viscosity modifying agent (VMA), and the impact of the water-to-binder (*w/b*) ratio. Additionally, the optimal flowability ranges, along with a rheological findings from previous studies on different types of 3DP-CC and 3DP-FRCC are also highlighted. This review paper will contribute significantly to a better understanding of this emerging technology by addressing all the fundamental aspects and will serve as a comprehensive guide for future researchers and industries engaged in the development of new 3D printable mixes.

2. Review methodology

The review methodology consisted of three primary stages: collection, screening, and critical evaluation of the literature. Initially, 'Web of Science' database was utilized to gather targeted papers for this review. The systematic search employed keywords such as '3DPC', '3DCP', '3D concrete printing', 'additive manufacturing', and 'Digital construction'. Subsequently, the collection was narrowed down to material science, and then further refined to focus only on studies related to cementitious composites. This resulted in 1212 research papers published between January 2016 to January 2024. Additionally, two more specific keywords, 'fresh property"' and 'rheology' were separately searched as this is the focus of this review, using the AND Boolean operator alongside the previously mentioned keywords. This refined search reduced the number of papers to 133. Only peer-reviewed papers, reviews, books, technical notes, and international standards and guidelines were retained, resulting in a final selection of 115 peer-reviewed works that met the criteria for the current review. These papers were then analysed one-by-one to understand all the aspects covered and summarized separately. Finally, all the summaries were cateorigsed based on the finalised section titles and added in the paper.

3. Flowability

The term *flowability* refers to the ability of a substance to move and remain stable under pressure while retaining its core properties [30]. Flowability is one of the most crucial fresh property parameters required for 3D printing of cementitious composites. If a cementitious composite does not exhibit sufficient flowability, it cannot be pumped through a nozzle effectively. Conversely, if a mixture possesses too much flowability, it won't retain its shape during printing. As per the previous literatures [31–33] related to 3DP-CC and 3DP-FRCC, flow table test is preferred to measure flowability using mini slump cone (50 mm height, 70 mm upper diameter and 100 mm bottom diameter) by applying of 25 table drops as per ASTM C1437 [34]. The spread diameter after 25 table drops is considered as the flowability of the respective mixture as shown in Fig. 2. This diameter should be in a particular range for the material to be 3D printable and the range usually is dependent on the mix parameters.

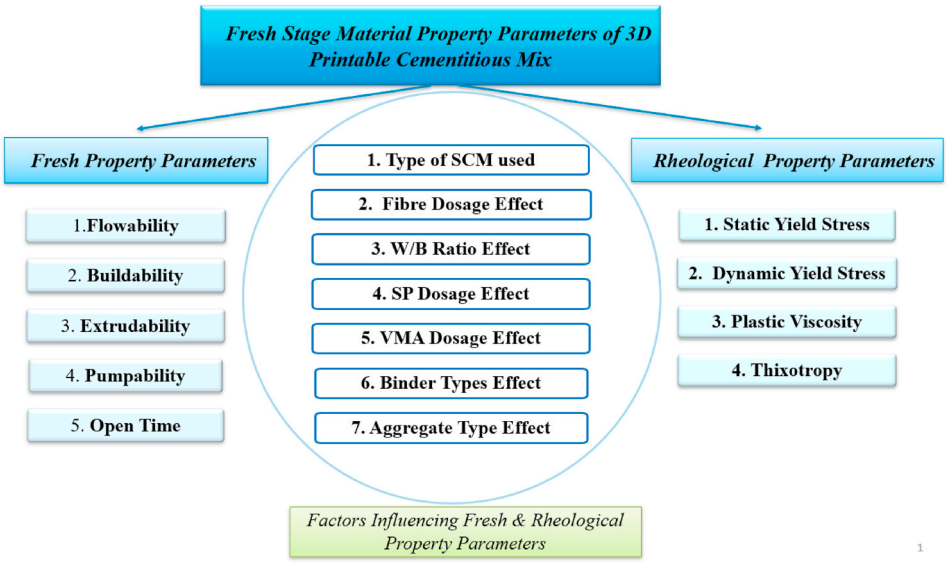

Fig. 1. Fresh and rheological property parameters of 3DP-CC and 3DP-FRCC covered in the present study.

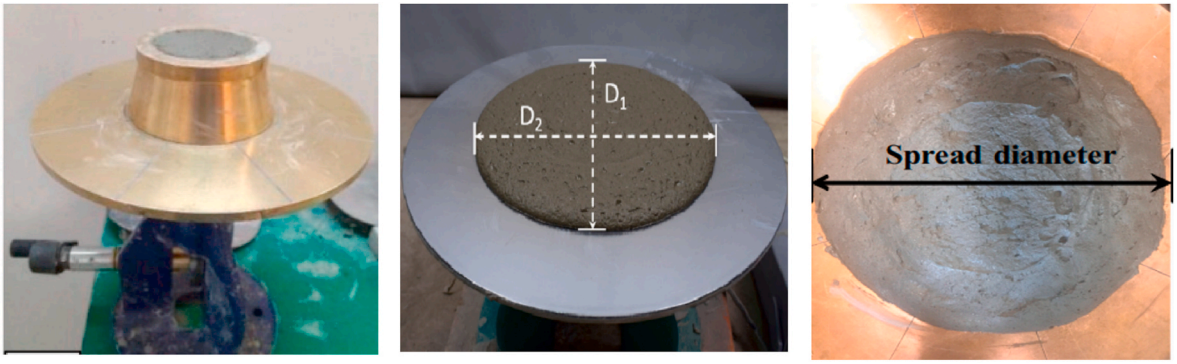

Fig. 2. Flow table tests conducted in previous studies.

3.1. Factors affecting flowability

3.1.1. Effect of type of SCM on flowability

The use of various SCM can have a significant impact on the flowability of a mixture. This is largely dependent on the properties of the SCM particles, which can vary depending on their mineralogical composition. Different types of SCM can exhibit different effects on various fresh property parameters, especially with regard to flowability.

1) Fly Ash (FA)

FA is the most extensively used SCM in 3D printing. Class F fly ash is mostly used in 3D printing which contains high levels of SiO_2 and Al_2O_3, but low amounts of CaO. It has smooth surface texture and is made up of fine particles ranging from 0.4 to 100 mm, with a low specific gravity (2.0–2.2 g/cm^3) and high specific surface area [35]. Due to having lower specific gravity than cement, when cement is substituted with FA, it increases the paste volume and reduces the concentration of cement, resulting in a reduction of flocculation. The round shape and smooth surface of FA particles aid in sliding and reduce friction, which is known as the 'ball bearing effect', especially when the particle size distribution is slightly coarser than cement. Due to this round shape and smooth surface, the addition of FA to cementitious mixtures has been reported to increase flowability [36]. Jalal et al. [37] reported that while using FA, it enhanced the slump flow diameter from 800 mm to 870 mm. Hajoti et al. [38] reported that mixtures with 50 % and 75 % binder replacement of FA required *w/b* ratios of only 0.26 and 0.24, respectively to achieve a flow diameter of 190–200 mm in a mini-slump test. The authors explained that the spherical shape of FA particles and their lubricating properties resulted in higher flowability and lower water requirement. The size of FA particles may also influence the flow behaviour. It was reported that as the size of FA particles increased, the slump flow decreased until it reached a certain value, after which it gradually increased again. The optimum particle size was found to be around 3 μm [39].

2) Ground Granulated Blast Furnace Slag (GGBFS)

GGBFS, a major byproduct of steel and iron industries, has a specific gravity similar to cement (2.5–2.9) and an absorption capacity of 1.2 %. Its composition is primarily CaO, SiO_2, and Al_2O_3 (up to 90 %), with hydraulic activity slower than Ordinary Potland cement (OPC). GGBFS has a grain size range of 1.18 mm–0.1 mm, bulk density from 1200 to 1670 kg/m^3, and a surface area of 4250 to 4700 cm^2/g, requiring more mortar for coverage, reducing paste available for lubrication and hence concrete flowability [40]. Zhao et al. [41] found that when 65 % of OPC was replaced with GGBFS, the flow diameter of the mortar increased by 45.5 %. This is due to the smooth and compact surface of GGBFS, which makes it less hydrophilic, resulting in less water absorption and more release of free water, ultimately enhancing the flowability of the associated mix design. Hajoti et al. [38] found that to achieve a flow diameter of 190–200 mm in a mini-slump test, mixtures with 50 % and 75 % binder replacement of GGBFS required *w/b* ratios of 0.33 and 0.32. It was further concluded that GGBFS requires more water compared to FA to attain the same flowability. According to research, replacing OPC with GGBFS can significantly improve concrete flowability. The optimal improvement is observed when there is a 40 % substitution ratio of GGBFS. However, beyond this ratio, the flowability improvement decreases [42]. When using more than 40 % GGBFS, superplasticizers are recommended to achieve necessary slump values. This is because the harsh surface texture and increased water absorption of GGBFS significantly impact concrete flowability.

3) Silica Fume (SF)

SF is a commonly used material that is added to cement mixtures to improve their performance in 3D printing. It is obtained as a by-product from the ferrosilicon and silicon industry and mainly consists of silica oxide, which typically makes up 89 %–97 % of its composition. SF contributes to the pozzolanic reactions that occur during cement hydration, which generates additional *C*–S–H gels and enhances the overall performance. It has an extremely fine powder consistency, with an average particle size of about 0.1–0.3 μm and a specific surface area ranging from 20,000 to 28,000 m^2/kg [40,43]. Generally addition of SF in replacement of OPC causes

reduction in flowability. According to Zhang et al. [44], in addition to SF, the flow value decreased compared to their control mix. Similar flowability reduction due to SF addition was also reported by Mahmood et al. [45]. Furthermore, Habibi et al. [46] found that increasing SF content from 0 % to 6 % resulted in a reduction in slump value from 85 mm to 65 mm. SF consists of particles much smaller than OPC, effectively filling the gaps between them. This phenomenon, often referred to as the filler effect, enhances the overall packing of the cementitious mixture. Additionally, SF has a lower specific gravity compared to cement. A high specific area with fine particle size creates higher water demand during the mixture process, thus it has a negative impact on the flowability [43].

4) Limestone Filler (LF)

LF is a by-product of the limestone quarry, and it has been used in cement-based materials for many years. LF is predominantly composed of calcium carbonate ($CaCO_3$). Its irregular and rough particle texture improves adhesion and friction between cement particles. The particle size of LF used in concrete varies from less than 1 μm to several tens of μm [40,47]. Barbosa et al. [48] found that adding LF significantly improved the flowability of the 3D printable mixture, and replacing 30 % and 40 % of OPC with LF resulted in flowability increase of 3.5 % and 5.9 %, respectively, as compared to the reference mix using 100 % OPC. Similarly, Teixeira et al. [49] found that LF mixed with *w/b* ratio of 0.43, resulted in a maximum flowability of 195 mm. However, a decrease in the *w/b* ratio to 0.39 led to a decrease in flowability to approximately 186 mm. The lower hardness of LF compared to clinker contributed to the increase in flowability as it led to a greater granulometric distribution, enhancing both the flowability and cohesion of the mixture. The fine LF filled the interparticle gaps, reducing water demand and increasing flowability. According to Camiletti et al. [50], LF enhances the flowability of the cement paste by releasing water that may be trapped between coarser particles, thereby increasing the available water content and contributing to greater fluidity.

5) Metakaolin (MK)

MK is a material made up of particles that are 99.9 % less than 16 μm in size, with an average particle size of approximately 3 μm. These particles are significantly smaller than cement grains but larger than SF particles by an order of magnitude. MK typically contains 50–55 % SiO_2 and 40–45 % Al_2O_3, with minor amounts of other oxides [51] The addition of MK generally results in reduced flowability. For instance, Camiletti et al. [50] reported 8.3 % reduction of flowability compared with the control mix with 100 % OPC after adding MK. Homayoonmehr et al. [52] also noted a similar trend of reduced flowability with MK, which they explained by highlighting higher specific surface area of MK that necessitated a higher *w/b* ratio, as well as an increased dosage of SP causing reduction in flowability.

3.1.2. Effect of fibre on flowability

The most common fibres which have been generally used as reinforcement in 3D printing are steel, polyvinyl alcohol (PVA), polyethylene (PE), and glass fibres. Typically, adding fibre results in decreased flowability. This is because increasing the amount of fibres enhances interlocking and further entangles the fibres in the mixture.

1) PVA Fibre

PVA fibre is type of synthetic fibre which has been commonly used in previous studies for making 3DP-FRCC. PVA fibre is cost effective as well as it improves the tensile strength of printed structures [53]. It increases the impermeability and impact resistance of cementious mix [21]. Sun et al. [54] conducted experiments with varying amounts of PVA fibres to assess their impact on flowability. They observed a clear decrease in flowability as the dosage of PVA fibres increased. Specifically, using 0.8 % by volume PVA fibre resulted in a 21 % higher flowability compared to increasing the dosage to 1.6 % by volume. Zhang and Aslani [53] also reported a similar decrease in flowability with the addition of PVA fibres. However, contrasting observations have also been reported on the effect of PVA fibre on flowability. For instance, Aslani et al. [55] reported that the incorporation of 1.75 % (volume percentage of binder) 12 mm PVA fibres enhanced the flowability comparing with the control mix without any fibre. They suggested that the addition of PVA fibre increased the segregation of mix components, leading to a higher level of flowability.

2) PE Fibre

PE fibre is another synthetic fibre commonly used to enhance ductility of 3DP-FRCC. PE fibre has shown significant strain hardening [56] and tensile performance [57]. PE fibres have hydrophobic properties which help in facilitating a multi-cracking behaviour. Like other fibres, the addition of PE fibre also reduces the flowability of the cementitious mix. Ye et al. [58] added 1 %, 1.5 % and 2 % (by volume of binder) PE fibre to a 3D printable engineered cementitious composite (3DP-ECC) mix and found that with the increase in the dosage of PE fibre, the flowability values significantly decreased. They found that increasing the fraction of volume of PE fibre from 1 % to 2 % resulted in a decrease in spread diameter from 169 mm to 144 mm and a decrease in slump depth from 86 mm to 76 mm, respectively. A recent study conducted by Bai et al. [59] used 12 mm PE fibres 0 %, 1 %, 1.5 %, and 2 % (by volume of binder) to investigate the printability and mechanical performance of proposed 3DP-ECC mix designs. It was found that as the fibre dosage increased (especially above 1 %), there was a decrease in spread flow diameter. The reduced fluidity of 3DP-ECC can be traced back to fibre overlap, which results in interconnected networks. Moreover, increased fibre concentration in the mortar impacts fluidity by expanding the surface area of the fibre-water interface. Similar outcomes were also reported by Zhang et al. [53]. The reason of reduced flowability was explained as the restriction caused by fibres against the movement of aggregates of the mixture.

3) Steel Fibre

Steel fibres are commonly used in 3DP-FRCC to enhance the structural integrity and durability of printed components. The

incorporation of steel fibers can significantly boost the strength, toughness, and strain capacity of concrete mixes, while also improving their energy absorption and resilience against fatigue and impact [21]. According to a study by Singh et al. [60], the addition of 13 mm long steel fibres resulted in reduced flowability as the fibre content increased to 0.25, 0.5, 0.75, and 1 wt percentage of the binder. In a similar study on the effect of steel fibres by Arunothayan et al. [61], it was discovered that adding steel fibres in volumes of 0 %, 1 %, and 2 % of the binder led to flowability values of 151 mm, 144 mm, and 127 mm, respectively. Yang et al. [62] discovered that omitting steel fibres led to better printing quality compared to mixes containing 1.0 vol % of steel fibres due to difficulties in extrudability when using steel fibres.

4) Other Fibres

Existing researchers have also used glass fibre, basalt or carbon fibre in 3DP-FRCC, however, the research is still in very early stage. Carbon fibers possess excellent resistance to corrosion, high temperatures, and fatigue, coupled with a favorable strength-to-weight ratio. They also have the potential to enhance the electrical conductivity and magnetic sensitivity of concrete. In contrast, glass fibers are known for their good heat insulation and corrosion-resistant properties [21]. Li et al. [63] utilized coral sand and seawater in the development of 3DP-FRCC, incorporating glass fibres. Their investigation showed that the addition of 0.6 vol percentage of glass fibre decreased the flowability of the mixture. A similar reduction in flowability due to the use of 0.5 vol percentage of glass fibres was also noted by Chu et al. [64]. The inclusion of basalt and carbon fibres have been noted to decrease the flowability of cementitious mixes. For example, Chu et al. [64] observed a 5 % decrease in flowability when adding 0.5 vol percentage of carbon fibres. Likewise, Li et al. [63] reported a reduction in flowability resulting from the addition of basalt fibre.

3.1.3. Effect of chemical admixtures on flowability

The use of chemical admixtures can significantly impact the flow behaviour of a cementitious composites. Adding SP, such as high-range water-reducing admixture, can increase flowability. Bohuchval et al. [65] studied the effects of SP dosage on flowability of 3D printable fresh mix. The study used a polycarboxylate polymer-based SP at two different levels, 0.136 kg/m^3 and 0.272 kg/m^3. The results showed that with an increase in the dosage of SP, the flowability value of the mix increased from 204 mm to 205 mm. Similar phenomena of increase in flowability with increase in SP dosage was also reported by Kwan et al. [66]. However, incorporating VMA, such as hydroxypropyl methylcellulose (HPMC), can decrease flowability. When the VMA dosage is increased, the viscosity of the mixture also increases, leading to a decrease in flowability. For instance, Zhu et al. [67] investigated the effects of adding HPMC on flowability of fresh ECC mixture reinforced with 2 % PE fibre. The study discovered that using HPMC resulted in a decrease flow table values from 176 mm to 155 mm respectively. Similar outcome of flowability reduction due to application of VMA was also found in the study conducted by Li et al. [68]. However, to achieve both optimal flow and adequate shape retention ability, it is necessary to balance the dosage of not only chemical admixtures but also the other mix constituents such as SCM and fibres.

3.2. Optimum flowability ranges for 3DP-CC and 3DP-FRCC

Different set of optimum flowability ranges have been reported for different 3DP-CC and 3DP-FRCC in respect of optimum printability. For instance, study conducted by Tay et al. [31] examined total 16 mortar based mix designs, taking into account different parameters like *w/b* ratios (0.45 and 0.55), sand to binder ratios (1.2 and 2.0), FA to binder ratios (0.10 and 0.20), and SF to binder ratios (0.08 and 0.12) with the slump flow values ranging between 108 mm and 212 mm. Initially, it was visually noted that a slump flow value below 130 mm made the material too stiff for smooth pumping, while a value above 210 mm resulted in excessive

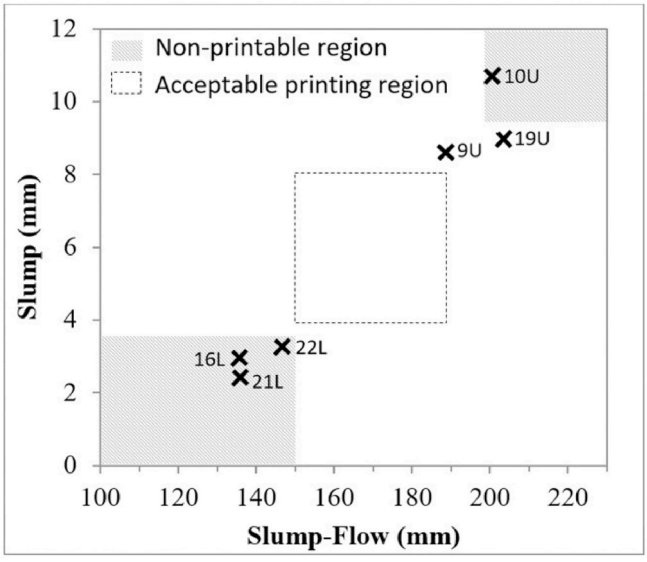

Fig. 3. Printable region for mortar as per flowability evaluation [31].

flowability, making it difficult to create a cohesive printed filament. Finally, 6 mix designs were further investigated for printability analysis having slump flow values ranging between 130 mm and 210 mm as shown in Fig. 3. It was observed that mixtures with slump flow values resulted in a rough surface texture, voids, and cracks, rendering the printed structure unstable and non-printable in the lower left shaded area of Fig. 3. On the other hand, mixtures with higher slump and slump flow values, while improving surface finish quality, hindered buildability when slump values were high, leading to a non-printable zone in the top right shaded area of Fig. 3. The study concluded that mixtures with a flowability value between 150 and 190 mm performed optimally for 3D printing, particularly in terms of extrudability and buildability, as illustrated in the square-shaped acceptable printability region in Fig. 3. Similar 3DP-CC based study was conducted by Hou et al. [69], wherein they used demolished brick and concrete powder to replace OPC by 10 %, 20 %, and 30 %. The investigation showed that the optimal range of flowability was between 160 mm and 220 mm, ensuring continuous extrudability without any crack formation. Another 3DP-CC based study conducted by Zhang et al. [70] incorporated 2 % SF and 2 % NC with OPC and found a higher flowability range of the fresh mixtures ranging between 192.5 and 269.0 mm. Similarly, the studies on 3DP-FRCC also present a different optimum range of flowability. For instance, according to Ma et al. [32], the ideal flowability range for FRCC was between 174 and 210 mm. The reported range of flowability values for different types of 3DP-CC and 3DP-FRCC are summarized in Table 2.

As per the recommended ranges of flowability values shown in Table 2, the overall average value was calculated to be 180 mm. Therefore, a general optimum flowability range suitable for printability can be defined as 160 mm–200 mm considering 10 % standard deviation as also shown in Fig. 4.

4. Buildability

Buildability, also known as self-retention ability, refers to the ability of an extruded layer to preserve its uniform shape despite being subjected to the self-weight of successive deposited layers. Structural build-up rate of a mixture is highly influenced by the rates of flocculation and hydration of the binders. If the rate of deposition for a layer is faster than the material's structurization rate, the layer will not be able to withstand and will fail eventually. Therefore, it is crucial to maintain a balance between the structural build up rate of the material and the number of layers to be printed in a certain duration of time keeping in consideration the layer dimensions and weight being imposed to bottom layers. The yield stress of a mix design in its fresh state is also crucial to its buildability performance. While buildability is a critical factor in evaluating the suitability of a cementitious composite design for 3D printing, there is currently no established criterion for assessing buildability. Indirect buildability test by imposing weight, layer deformation test and maximum layer print counting test are the most extensively used test methods used to assess buildability in previous literature both for 3DP-CC and 3DP-FRCC. Various buildability measurement methods are briefly described below.

4.1. Indirect buildability test by imposing weight

This test method does not involve direct printing through a 3D printing machine. Rather, it uses an indirect method to identify buildability by measuring the spread diameter of a fresh sample at an imposed weight. The weight would depend upon the number of targeted numbers of printing layers as well as on the unit weight of the material. Yu et al. [33] assessed the buildability of engineered cementitious composite (ECC) mix designs by adding a 600 gm weight to the fresh mix design and calculating the spread diameter of the fresh mixture after 1 min of continuous load application as shown in Fig. 5 (a). Here, the weight of 600 gm was adopted which was roughly equivalent to the weight of three layers placed on top of the bottom layer. It was found that with the increase of time after water addition, the spread diameter reduced indicating higher shape retention ability. With the prepared mix design, a twisted column of 150 layers with 1.5 m height was successfully printed at 20 min rest time. Nematollahi et al. [74] conducted a test where they used a

Table 2
Optimum flowability ranges for 3DP-CC and 3DP-FRCC reported in literatures.

Reference	SCM type – dosage (%wt. of cement)	Fibre type and dosage (% vol.)	Fibre length, L (mm), diameter, φ (μm)	Flowability Range (mm)
[31]	FA - 10, 20 SF - 8, 12	–	–	150–190
[69]	RP - 10, 20, 30	–	–	160–220
[70]	NC - 2, SF - 2	–	–	192.5–269
[71]	None	–	–	180–240
[49]	50 % LF 40 % LF + 25 % FA 25 % LF + 25 % MK	–	–	186–198
[32]	FA- 20 SF -10	PP- 0.13	L - 9 φ - 23	174–210
[72]	FA- 75	PVA- 1.2	L - 8 φ - 39	120–132.5
[61]	SF- 30 % NC- 0, 0.1 %, 0.2 %	SE - 0, 1, 2	L - 6 φ - 200	125–130
[59]	FA- 40, SF- 10	PE – 0, 1, 1.5, 2	L - 12 φ - 24	180–190
[73]	None	PP- 0.15 % of cement wt.	L - 6	165–180.5

Note: FA- Fly Ash, SF- Silica Fume, NC- Nano Clay, LF- Limestone Filler, MK- Metakaolin, RP- Recycled Powder (demolished brick and concrete waste powder), PP – Polypropylene Fibre, PE- Polyethylene Fibre, PVA- Polyvinyl Alcohol Fibre, SE- Steel Fibre.

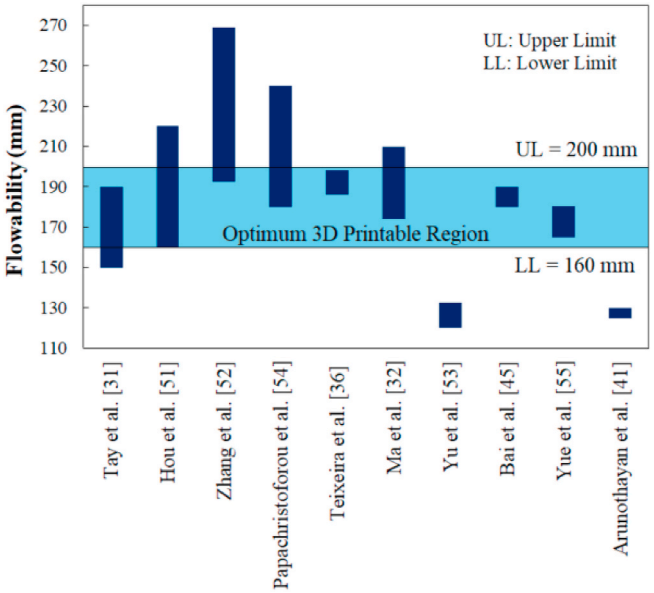

Fig. 4. Optimum flowability range analysis as per previous literature.

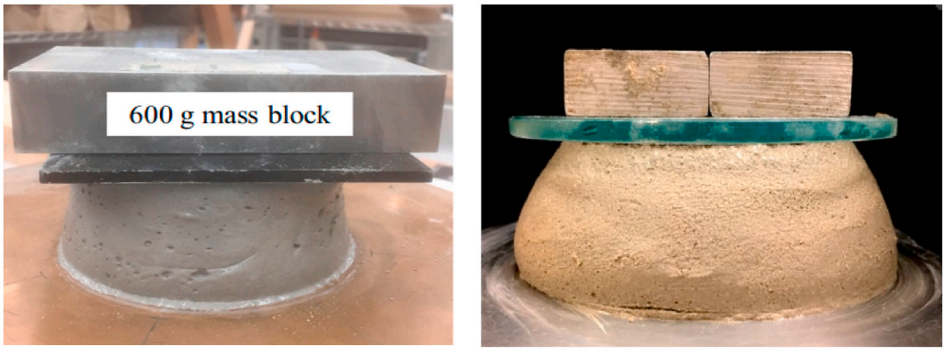

a) Applying a 600g mass load for one minute [33]

b) Spread diameter after 600 gm load application [74]

Fig. 5. Indirect buildability test.

Table 3
Indirect buildability test results.

Reference	SCM type – dosage (%wt. of cement)	Fibre type and dosage (in % vol.)	Fibre length, L (in mm), Diameter, φ (in μm)	Load (gm)	Time of test (min)	Spread Diameter (mm)
[33]	FA (75 %)	PVA- 1.2	L - 8 φ - 39	600	20 40 60 80 100	106 105 103 102 101
[74]	FA based geopolymer	PP – 0, 0.25, 0.50, 0.75, 1	L-6 φ - 11.2	600	–	144 (0 % PP) 124 (0.25 % PP) 121 (0.50 % PP) 120 (0.75 % PP) 112 (1 % PP)

Note: FA- Fly Ash, PP – Polypropylene fibre, PVA- Polyvinyl Alcohol fibre.

100 gm glass plate on top of the raw mix surface. Two metal weights totalling 500 gm were then placed on top of the glass plate to distribute the weight evenly over the entire cone surface as shown on Fig. 5 (b). In this study, PP fibre was used at 0.25–1% and it was clearly found that addition of fibre enhanced the buildability. The indirect buildability-related results are further summarized in Table 3 showing the effect of fibre and test time on buildability. It is evident from Table 3 that the spread diameter while imposing load gets reduced with an increase in rest time [30]. Similarly, an increase in fibre content reduces weighted spread diameter indicating development of buildability performance [74].

4.2. Layer deformation measurement method

Buildability can be calculated by layer deformation method computing the average vertical strain of the printed layers. For this method, direct printing of layers using 3D printing machine is required. Zhou et al. [67] determined the buildability of their prepared mix deigns by printing box shaped structures of 300 mm height. The total height and individual filaments thickness were measured at the four edges and thereafter, average vertical strain (AVS) was calculated as shown in Fig. 6. With AVS, the resistivity of a printed material against the deformation caused by self-weight was further determined which was directly used as an indication of buildability. The buildability decreased as the AVS value increased. The AVS (ε_v) was calculated using Equation (1).

$$\varepsilon_v = 1 - \frac{(H - h_1 - h_n)}{(n-2)h_0} \tag{1}$$

Similarly, Ma et al. [32] printed 20 layers and assessed the buildability by analysing the overall AVS of the printed layers. Similar buildability analysis was conducted by Zhu et al. [57]. They printed hollow cylindrical models of 260 mm diameter and 221 mm height to test the buildability of PE fibre-reinforced 3DP-ECC mix design. Each model contained 17 layers with 13 mm thickness. Three dimensionless parameters related to vertical strain from the printed layers were analysed, and the overall shape retention capability was quantified. Barbosa et al. [48] determined the buildability using LF and MK based mortar mixes by printing 400 mm long layers overlapped with 5 layers and buildability was evaluated by the buildability ratio (H_B) between the real height of the 5 stacked layers by the theoretical predicted height of 5 layers as shown in Equation (2). Higher the H_B value implied higher amount of buildability.

$$H_B = \frac{H_R}{H_T} \tag{2}$$

Here, H_R and H_T represent the measured height of 5 layers and the theoretically expected height of the 5 layers, respectively. The maximum attainable value for H_B is 1, indicating a zero deformation.

A dimensionless parameter representing the layer deformation λ is also used to determine buildability as defined in Equation (3) [75].

$$\lambda = \frac{\sum_{i=1}^{n} \Delta L_i}{nL} \times 100\% \tag{3}$$

where, n represents counting times, ΔL_i is the offset or deformed height, and L is the theoretical height value for each layer, respectively. A lower λ value indicates a higher ability of the mixtures to retain their shape. Test results of several layer deformation methods for buildability evaluation are summarized in Table 4. It is evident that AVS value for printable mixes including different dosage of fibres reported roughly between 0.3 % and 4.3 %. Along with AVS, buildability ratio between layers of 0.70 to approximately 1 have been measured to compare the buildability performance between several investigated mixes.

Fig. 6. Buildability test by layer deformation method [67].

Table 4
Layer deformation method test results.

Reference	SCM type – dosage (%wt. of cement)	Fibre type and dosage (in % vol.)	Fibre length, L (in mm), Diameter, φ (in μm)	Test parameter	Range (%)
[67]	FA – 45 %, SF – 10 %	PE-1	L –12 φ - 24	AVS	1.6 %–0.3 %
[32]	FA - 20 % SF – 10 %	PP- 0.13	L - 9 φ - 23	AVS	2.5 %–0.75 %
[57]	SAC- 3 % FA- 57 %	PE – 1, 1.5, 2	L - 12 φ - 24	AVS, Layer width strain (W), Outer diameter strain (φ)	4.3 %–0.8 % (AVS) 26 %–5.5 % (W) 8.3 %–0.7 % (φ)
[48]	LF-30 %, 40 % MK-10 %	–	–	Buildability Ratio, H_B	0.70–0.95
[75]	No SCM	–	–	Offset percentage	16.3%–1.13 %
[71]	FA-20, SF-10 GGBFS- 20, SF-10	–	–	Ratio between 1st and 5th layer	~1

Note: FA- Fly Ash, SF- Silica Fume, LF- Limestone Filler, MK- Metakaolin, PP – Polypropylene fibre, PE- Polyethylene fibre, SAC- Sulfoaluminate cement, AVS-average vertical strain.

4.3. Maximum continuous print height or layer count method

The most direct method to assess buildability which can be even visually monitored is the maximum continuous layer count method (MCLC). In this method, continuous printing of layers is required until there is a collapse of printed layer. The evaluation of buildability is then based on either counting the total printable layers or determining the maximum continuous print height (MCPH). Zhou et al. [67] explored the impact of various printability parameters and achieved successful printing within a range of 25–30 layers depending on the parameters being considered for their 3DP-ECC mix design. Bai et al. [59] prepared 3DP-ECC mix design and could build total 945 mm high printed layers. Tay et al. [59] could print up to 28 layers as shown in Fig. 7 (a) and Yue et al. [31] could print up to 17 layers with their investigated mix design as shown in Fig. 7 (b). A short summarization of buildability determination analysing previous literatures by MCPH and MCLC methods are shown in Table 5.

It is clear from Table 5 that various SCM have different effects on the overall printability. For example, incorporating 2 % NC and 2 % SF could print could result in print heights ranging from 72 mm to 260 mm [44]. On the other hand, mix design with 50 % FA and 10 % SF, incorporating PE fibre with 1 %, 1.5 %, and 2 % dosage of volume of binder can significantly enhance the print height up to 945 mm [81]. In terms of layer counting for 3D printing, previous studies have indicated that the maximum number of layers can vary widely (zero to more than 320 [79]) depending on the specific mix design used. Factors such as the type and amount of SCM used, the inclusion of fibres, and the use of chemical admixtures can all impact the maximum achievable layer count.

4.4. Factors affecting buildability

4.4.1. Effect of SCM on buildability

Both NC and SF have been widely used to improve buildability [44,82]. Zhang et al. [44] found that the incorporation of SF and NC

Fig. 7. Buildability evaluation by MCPH and MCLC.

Table 5
MCPH/MCLC based buildability test results.

Reference	SCM type – dosage (%wt. of cement)	Fibre type and dosage (in % vol.)	Fibre length, L (in mm), Diameter, φ (in μm)	Test parameter	Maximum Number of layers/print height (mm)
[44]	NC - 2 % SF - 2 %	–	–	MCPH	72–260 mm
[76]	WGP- 0 %, 20 %, 40 %, 60 %	–	–	MCPH	150–155 mm
[77]	GGBFS- 60 % SAC- 10 %	–	–	MCPH	41.7–113 mm (at 50 min) 125.5–138 mm (65 min)
[78]	SCA-5% SF-5% FA-22 %	–	–	MCLC	0-50 layers
[69]	RP- 10, 20, 30	–	–	MCLC	11-13 layers
[79]	SF-10	–	–	MCLC	21-320 layers
[80]	FA – 20 % SF – 10 %	–	–	MCLC	15–61 layers
[31]	FA - 10 %, 30 %, SF – 8 %, 12 %	–	–	MCLC	19-28 layers
[61]	SF- 30 % NC- 0, 0.1 %, 0.2 %	Steel fibre- 0, 1, 2	L - 6 φ - 200	MCLC	50 layers
[81]	FA – 50 %, SF – 10 %	PE - 1, 1.5, 2	L –12 φ - 24	MCPH	945 mm
[73]	None	PP- 0.15 % of cement wt.	L - 6	MCLC	13-17 layers

Note: FA- Fly Ash, SF- Silica Fume, NC- Nano Clay, GGBFS- Ground Granulated Blast Furnace Slag, SAC- Sulfoaluminate Cement, WGP- Waste Glass Powder, RP- Recycled Powder (demolished brick and concrete waste powder), PP – Polypropylene Fibre, PE - Polyethylene Fibre, MCPH- Maximum Continuous Print Height, MCLC- Maximum Continuous Layer Count.

both increased the buildability. The control mix design demonstrated a buildable total extruded layer height of only 72 mm. While individually, 2 % SF and 2 % NC additives increased build height to 156 mm and 180 mm, respectively, the combined incorporation of both 2 % SF and 2 % NC enabled the maximum buildability height of 260 mm. Similarly, Jayathilakage et al. [79] reported the effectiveness of using NC to enhance buildability. The study found that incorporating only 0.1 % or 0.3 % of NC significantly improved buildability. With these amounts of NC, the material could be printed up to 160 to even more than 320 layers, respectively. In contrast, the control mixture without any NC could print only up to 21 layers before becoming damaged, as depicted in Fig. 8. Arunothayan et al. [61] also reported that the addition of NC showed a significant improvement in buildability performance. Out of the three NC dosages tested (0 %, 0.1 %, and 0.2 %), only 0.2 % dosage was able to maintain satisfactory buildability across all printing speeds (30 mm/s, 50 mm/s, and 80 mm/s). It is important to note that using too much NC can result in issues like filament blockages or tearing, which can

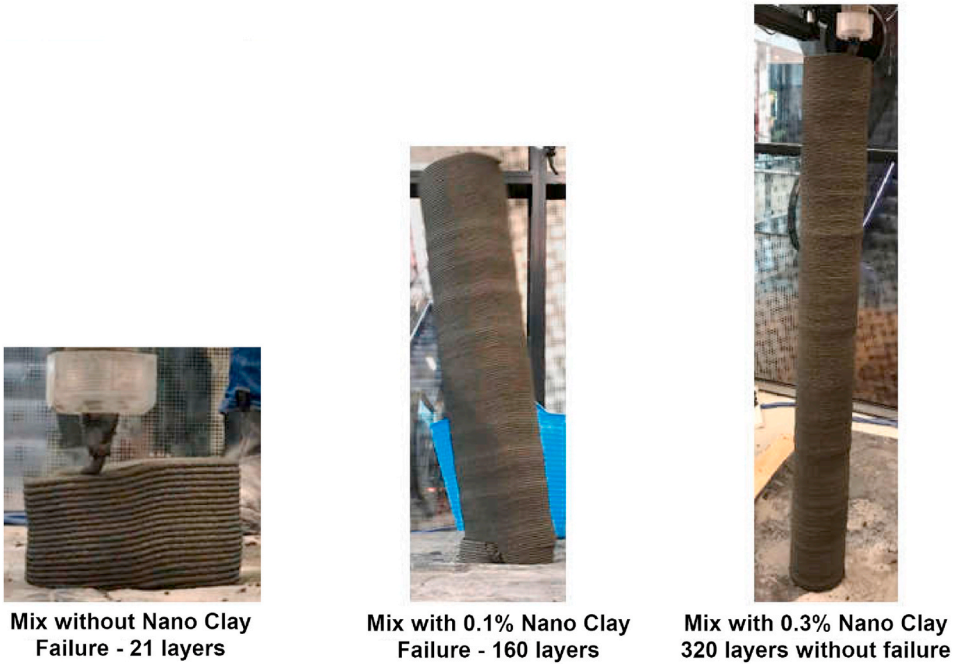

Fig. 8. Effect of NC dosage on buildability [79].

negatively impact the extrusion process [82].

LF, on the other hand, exhibits opposite effect on buildability in comparison with NC and SF. Barbosa et al. [48] found that in comparison with the reference mortar without any SCM, the inclusion of LF decreased buildability performance. Notably, as LF content increased from 30 % to 40 %, the buildability ratio decreased from 0.79 to 0.70. Conversely, the addition of MK positively impacted buildability. With just 10 % MK added to the previous 30 % LF mix, the buildability ratio increased from 0.79 to 0.95, signifying an approximately 20 % enhancement in buildability.

4.4.2. Effect of fibres on buildability

With increasing fibre dosage, buildability improves for all types of fibres generally employed in 3D printing such as steel fibre, PVA fibre, PE fibre, basalt fibre etc. A higher concentration of fibres generally leads to increased interlocking and entanglement among fibres in mixtures, which restricts fluidity and enhances shape retention ability or buildability. Arunothayan et al. [61] found that increasing dosage of steel fibre improved the buildability. Specifically, it was found that 2 % steel fibre and 0.2 % NC employment in the mix allowed to print 50 consecutive layers. Furthermore, Ye et al. [58] observed that when printing a 10-layered structure, the height variations were 99 mm and 97 mm for 2 % and 1 % PE fibre addition, respectively. Li et al. [63] also reported that the buildability height of the prited structure was increased from 52.3 to 52.5 mm by incorporating 0.85 % volume of basalt fibre.

4.4.3. Effect of chemical admixtures on buildability

SP and VMA have completely opposite effect on the buildability. While SP dosage increment enhances the flowability of a mix, overdosage of SP may deteriorate the buildability performance. As per the study conducted by Souza et al. [83], it was reported that the addition of 0.1 % polycarboxylate ether-based SP enhanced the buildability performance of cement paste, whereas 0.3 % dosage made the mix too much flowable. However, no detailed study on the optimization of SP dosage in respect of attaining desired buildability has been conducted. In contrast, optimized VMA dosage can help to enhance the buildability performance. HPMC is used as a thickening agent in printable cementitious mixes to improve their shape retention after extrusion. It also helps to prevent the segregation of raw mix. Chen et al. [84] conducted tests to measure the effect of VMA on buildability, and they found that the addition of VMA improved the buildability performance. However, excessive dosage of VMA was found to delay cement hydration. It was concluded that 0.24 % of VMA (by binder weight) exhibited optimum printability performance. Soltan et al. [85] also found positive

a) 8 continuous filament printing [32]

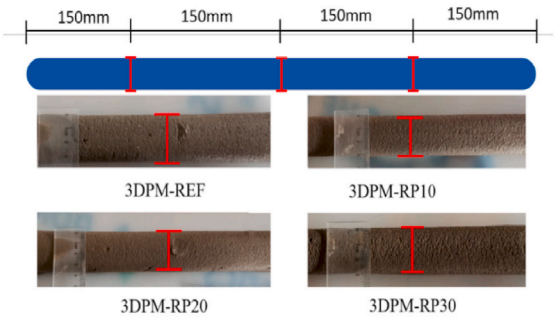

b) Continuous print and width measurement [69]

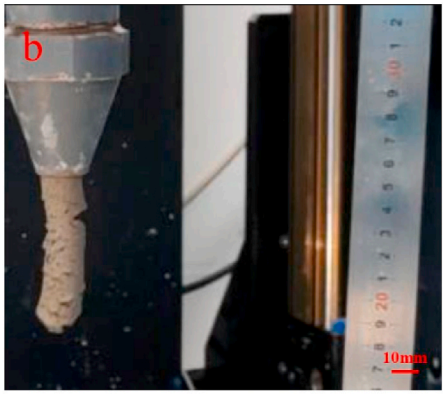

c) Continuous printing till fracture [89]

Fig. 9. Extrudability tests by filament printing in previous literatures.

effects of using HPMC in the their mix design. It was reported that 0.4 % (volume fraction of total binder) HPMC helped in controlling viscosity which ultimately enhanced the buildability. Similarly, Zhu et al. [63] investigated the effects of adding HPMC on the fresh properties of a 3DP-ECC based mixed design reinforced with 2 % PE fibre. The study discovered that HPMC improved the shape retention capacity.

Yin et al. [77] also conducted a thorough investigation into the impact of HPMC on the rheological properties of 3D printable mortar. They observed a significant improvement in buildability when HPMC was used. The reference mix without HPMC struggled to accumulate layers for approximately 50 min of hydration time. However, with the addition of HPMC, the static yield stress and viscosity of the fresh mixes increased. As the HPMC content varied from 0.05 % to 0.2 %, the initial buildable height also increased. For instance, at 0.2 % HPMC, the extrudate could accumulate up to 66 mm in height which was zero for the corresponding reference mix without any HPMC. Notably, the width deviation decreased from 500 % in the reference mix without HPMC to only 8.33 % with a 0.2 % HPMC dosage. This enhancement allowed the mix to accumulate 11 layers within just 5 min of hydration, a feat impossible for the reference mix without HPMC which struggled even to extrude a single layer properly. In summary, the optimization of chemical admixture dosage is crucial for achieving desired buildability, as overdosage of VMA or SP may have adverse effects on buildability.

5. Extrudability

Extrudability is used to describe the capability of a 3D printable mixture to maintain dimensional precision and layer quality while continuously extruding from the nozzle [86–88]. Achieving accurate and precise 3D printed structures with 3DP-CC mix largely depends on its ability to be extruded appropriately. Proper extrudability is necessary for desirable build quality. There is currently no standardized method for determining the extrudability of a mix. However, to measure the extrudability of 3DP-CC and 3DP-FRCC, printing is done directly with the respective material in its fresh state. The total length of the material that can be printed without any breakage or interruption, while maintaining good surface smoothness, is then measured. The higher the uninterrupted length during printing, the higher its extrudability.

Ma et al. [32] determined extrudability by printing 8 subsequent continuous filaments, each 250 mm long, to create 2000 mm long layers. After printing, the layers were visually inspected for continuity and stability, as shown in Fig. 9 (a). Similarly, Le et al. [80] developed a method to test the extrudability of mixtures. They utilized filaments that were 9 mm in width and 300 mm in length. The approach entailed assessing the geometric deviation between the nozzle and the printed filament. Hou et al. [69] printed 600 mm filaments for each mix design and measured its width at 3 different points to determine its average width. This was used to evaluate the extrudability of the filament, as depicted in Fig. 9 (b). Xu et al. [89] tested extrudability at a printing speed of 2 cm/s, measuring the length until fracture using their 3D printable mixes as shown in Fig. 9(c).

Ram extruders have also been used in previous studies to evaluate extrudability. Varela et al. [90] used a ram extruder in conjunction with a universal testing machine that had a 5-kN load cell. The extrudability test was performed 10 min after introducing water to the dry mix. An analysis of force versus displacement was performed for various mix combinations. The extrudability outcomes were classified into two categories: (a) proper extrusion, characterized by an initial maximum peak followed by a force reduction due to reduced friction surface, and (b) deficient extrusion, marked by a notable force increase (frictional behaviour) after the initial peak. Tay et al. [31] conducted a study on 3DP-CC based mix design to determine favorable slump and slump-flow values to get optimum extrudability as well as buildability. The extrudability test was separately conducted by a 3D printing machine. After analysing the results, they plotted them on a slump and slump-flow diagram to identify the appropriate range for extrudability and buildability. The ideal range for slump values of extruded mortar specimens was found to be between 4 and 8 mm, while the preferred slump-flow diameters ranged from 150 to 190 mm. Different extrudability testing results are also summarized in Table 6 which further reveals that the extrudability performance is mostly assessed by visually observing the printing of filaments with different geometric configurations and lengths ranging from 40 mm [89] to 600 mm [69]. The adopted length of filament for testing depends on the printer and observation strategy.

Table 6
Different extrudability tests conducted in previous literatures.

Reference	SCM type – dosage (%wt. of cement)	Fibre type and dosage (in % vol.)	Fibre length, L (in mm), Diameter, φ (in μm)	Test parameter	Filament length and geometry
[89]	SAC-10 FA- 0, 10, 20, 30, 40 GGBFS- 0, 10, 20, 30, 40	–	–	Uninterrupted length	40–62 mm
[69]	RP - 10, 20, 30	–	–	Uninterrupted length and average width	Filament length- 600 mm, Width range 2.95 cm–3.45 cm
[80]	FA – 20 SF – 10	PP – 0.13	L - 12 φ - 18	Uninterrupted length	300 mm long – 5 continuous filament printing
[32]	FA- 20 SF -10	PP – 0.13	L - 9 φ - 23	Visual observation of continuity	250 mm long – 8 continuous filament printing

Here, FA- Fly Ash, SF- Silica Fume, GGBFS- Ground Granulated Blast Furnace Slag, RP- Recycled Powder (demolished brick and concrete waste powder), PP – Polypropylene Fibre, PE - Polyethylene Fibre.

5.1. Factors affecting extrudability

5.1.1. Effect of SCM and fibre on extrudability

According to a study conducted by Xu et al. [89], the effects of adding FA and GGBFS to the mixture were examined to determine their impact on extrudability. The study found that increasing the FA content improved the extrudability. The use of 10 %, 20 %, and 40 % of FA in place of OPC demonstrated uninterrupted extruded lengths of 50 mm, 91 mm, and 85 mm, respectively. Thus, the best replacement dosage of FA was found to be 20 % in terms of extrudability and surface smoothness, while a higher dosage weakened the extrudability property. GGBFS also showed similar effects. The study found that increasing the GGBFS replacement percentage from 0 %, 20 %, and 40 % resulted in an increase in fracture length from 40 mm to 98 mm, which eventually decreased back to 62 mm. Optimum dosage of GGBFS was found to be 20 %, considering surface smoothness as well as uninterrupted length. The process of extrusion, particularly for 3DP-FRCC, plays a significant role in the final deposited material because it determines the ultimate orientation of the fibres. It is commonly observed that when fibres are transported by the fluid mixture in printed specimens, they align themselves longitudinally with the filament [91]. Figueiredo et al. [92] revealed that when extruding fibres, they tend to align diagonally, resulting in a V-shaped pattern behind the nozzle. The flow at the print head exit was not found to be uniform, which caused varying flow velocities when the fibre orientation was at an angle greater than 45° to the filament direction. However, the existing studies on the effect of fibre are very limited and further research is needed to evaluate the impact of fibre type and dosage on extrudability properties.

5.1.2. Effect of chemical admixture on extrudability

The dosage of SP and VMA can also impact the extrudability performance of 3DP-CC and 3DP-FRCC. Rahul et al. [93] investigated the impact of polycarboxylate ether (PCE) based SP dosage on the extrudability of mortars. They discovered that using less than 0.09 % SP caused blockages in the nozzle during extrusion but using 0.10 % allowed for smooth extrusion without any interruptions. Yin et al. [77] assessed the effect of VMA and found that the addition of HPMC to mortar mix can improve its extrudability. The reference mix without HPMC was unable to achieve extrudability at 5 min of hydration time, and only reached proper extrudability at 65 min. However, with a small addition of HPMC (0.10 %, 0.15 %, and 0.2 %), the extrudability was highly improved even at just 5 min of hydration time. These findings illustrate that HPMC possesses the capacity to improve the printing precision of the initial layer, a crucial element for successive 3D printing and the entire printing procedure. Similarly, Hou et al. [69] found that the addition of HPMC in 3DP-CC enhanced viscosity and reduced the swelling of free water, thus positively contributing to better extrudability performance. These findings were further supported by Zhou et al. [57]. Varela et al. [90] compared the behaviour of different VMAs and concluded that among polyacrylamide and methylcellulose VMA, methylcellulose showed a remarkable contribution to improving yield stress, cohesion, and overall extrudability of fresh mixes. Overall, optimizing the dosage of SP and VMA can be a useful tool in achieving the desired amount of extrudability. It should be noted that sand to binder ratio should also be taken into consideration while optimizing the dosage of SP and VMA to achieve best extrudability. Le et al. [39] observed that higher ratios of sand to binder caused blockages in pipes due to the separation of the mixture during extrusion. Furthermore, it was reported that minimum 0.9 kPa of static yield stress was required for achieving acceptable extrudability. Ogura et al. [56] also showed that the ease of extrusion in 3DP-ECC is higher when the sand/binder ratio is lower.

5.1.3. Effect of printing parameters on extrudability

The pumping pressure plays a significant role in maintaining the extrudability, especially when the printer head changes direction. Extrusion speed and mortar flow rate are also significant factors that impact the quality of extrusion. To ensure successful extrusion, it is essential to synchronize the extrusion speed with the flow rate. Additionally, the distance between the pump and nozzle also affects the extrudability properties. Based on research conducted by Xiao et al. [94], performing 3D printing on a larger scale may result in issues such as segregation, discontinuity, and instability in the filaments. This is due to the greater distance between the concrete mixer and the extrusion unit, resulting in significant changes in fresh material rheology during the extended pumping process. Zhao et al. [95] found that the extrusion speed and feed speed have a significant impact on the extrudability of fresh mix. When the feed speed and rheological parameters remain constant, an increment in extrusion speed results in an enhancement in the width of the printed strip. The study recommended extrusion speed to feed speed ratio to be maintained between 4 and 5 to get optimum extrudability.

6. Pumpability

Pumpability refers to the ability of a mixture to be pumped under pressure through a conduit. Ideally, the mixtures should have a smooth consistency and low viscosity during the pumping process. Currently, there is no established testing procedure to measure pumpability. However, a fresh cementitious mix that demonstrates satisfactory flowability is typically expected to show good pumpability. If the pumping process is interrupted, the raw material inside the pump and pipelines begins to solidify, making it difficult to pump out the remaining raw materials and increase the chance of clogging.

Tay et al. [31] introduced the concept of pumpability index, a dimensionless parameter that estimates pumpability of 3D printable mortar. To calculate the index, the flow rate of the mixture through the pump is measured and is compared to the flow rate of water at 2869 rpm. The index was found directly proportional to flowability, with the increase of flowability the index value also was increased. In another study conducted by Figueiredo et al. [96], the pumpability of various 3DP-FRCC mix designs was evaluated using a pumping unit connected to a 5-m long hose with a diameter of 25 mm. The measurements were conducted using the standard print nozzle, which has a mouth opening of 40 × 10 mm, to determine if the material can be smoothly pumped and effectively transported through the hose, without clogging. Correlations between pumpability, rheology and buildability was proposed by Weng et al. [97] considering

3DP-FRCC as show in Equations (4) and (5) below.

$$H = \frac{\alpha}{\rho g}\,\tau(t) \tag{4}$$

$$P = \left[\frac{8\tau(t)}{3R} + \frac{8k(t)}{\pi R^4}Q\right]L \tag{5}$$

where, H and P represents printed height and pumping pressure, respectively. R, L and Q indicates hose pipes radius, length and flow discharge rate. ρ and g represent the density of the mixture and gravitational constant.

6.1. Factors affecting pumpability

6.1.1. Effect of SCM on pumpability

Among the various types of SCMs, SF has been found to be highly effective in improving the pumpability of any cementitious mixture. The addition of SF helps in increasing the thickness of the slip layer, which in turn reduces the flowability of the mixture [14]. It was further reported that SF has a significant impact on the thickness of the lubricating layer in comparison to GGBFS and FA [98]. This may be due to the relatively smaller size of the SF particles. FA has a lower specific gravity compared to cement, which leads to an increase in paste volume. The smooth surface and round shape of FA particles promote sliding and reduce friction among them, known as the "ball bearing effect." The inclusion of FA particles improves flowability by increasing packing density and reducing water trapped in particle flocs and overall increases pumpability [99]. Similarly, the inclusion of GGBFS can decrease the plastic viscosity of cementitious mix, which may be attributed to increased pumpability [89].

6.1.2. Effect of chemical admixture and fibre dosage on pumpability

Proper adjustment of chemical admixtures such as SP and VMA, along with the fibre dosage, is vital for pumpability performance. As the fibre dosage increases, the mix becomes more stiff and less flowable, which ultimately requires more pumping pressure to be extruded out. However, appropriate adjustment of SP and VMA may reduce water bleeding, leading to good pumpability. Nonetheless, further investigation is necessary regarding the addition of fibre and chemical dosage adjustment in the context of pumpability. A study conducted by Yin et al. [77] found that the addition of HPMC to mortar mix leads to improved cohesion and pumpability of the mix. The study found that HPMC enhances the pumpability of the mix by three ways. Firstly, it increases the extrusion force, which improves the pumpability. Secondly, it delays hydration reactions, resulting in an extended open time, which is desirable for 3D printable mixes. And lastly, HPMC enhances the cohesion of the 3D printable mix, which is essential for precise printing according to the desired plan.

7. Open time

Open time is another important printability parameter of a 3D printable mix. The duration of the open time should be sufficient to allow for proper extrusion and effective printing. Once the dry mix components are mixed with water, the open time ends when it is no longer possible to extrude fresh mix that maintains precise dimensions and pumpability. Failing to accurately determine the open time can lead to reduced filament width and, eventually, the inability to produce continuous filaments. Ma et al. [32] examined the open time by calculating the maximum period during which their material can be extruded without experiencing any breakage. To calculate the open time, they extruded a 250 mm filament at 5-min intervals and monitored for any interruptions or breakages in the extruded filaments, as shown in Fig. 10. The end of open time was determined once the extrusion was no longer smoothly continuous and showed breakage. A similar method has been used by Chen et al. [100] to determine open time. Kazemian et al. [101] and Panda et al. [102] further showed that the open time always occurs before the initial setting time, even though there is no direct correlation between them. Therefore, it can be roughly assumed that a longer initial setting time leads to a longer open time. Using this concept, Bakhshi et al. [38] indirectly predicted the open time of 3D printable ECC by calculating the initial setting time of the mixtures.

It should also be noted that open time can directly be related with the flowability. With a view to determine the open time of a mix, its flowability can also be measured over a set of time periods. Yu et al. [33] conducted flow table test and indirect buildability tests to

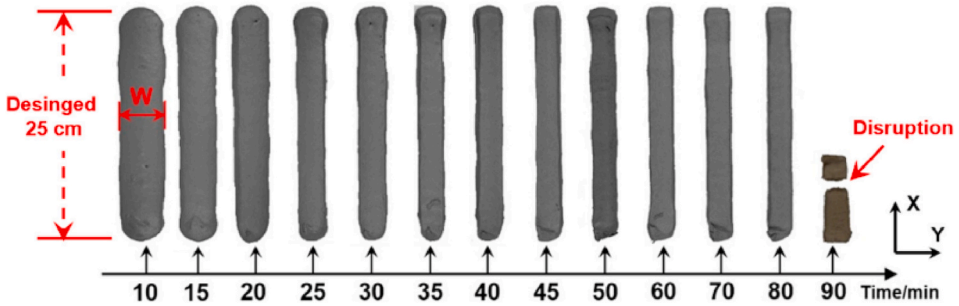

Fig. 10. Open time determination through extrusion process [32].

determine the open time for a 3DP-ECC mix design. They found that the ideal open time was 70 min after adding water, which allowed for a balance between pumpability and buildability. Le et al. [80] reported that once there is a 0.3 kPa increase in shear strength compared to the initial level, this indicates the end of the open time.

Open time can be signifincally influenced with the use of suitable retartders. Retarder plays a crucial role in preventing the structurization of cementitious composites, causing delay in setting time, and enabling easy movement materials from the pumping unit to the extruder unit. Le et al. [80] found that using a 0.5 % dosage of the retarder resulted in achieving 100 min of open time. Chen et al. [103] also reported similar outcome and found that utilization of retarder increased the initial setting time and open time for printing. It is further important to note that open time is highly dependent on the SCM used. For instance, utilization of GGBFS as SCM not only facilitates early strength gain, but also reduces open time [104]. Moreover, higher concentrations of GGBFS tend to cause the mixture to set quickly, resulting in a shorter open time in comparison with FA and SF [38]. Addition of LF can also increase the open time in comparison with the reference mix without having any SCM. Conversely, the addition of MK was observed to reduce the open time, requiring a higher dosage of SP to achieve a comparable open time as that resulting from LF. In general, the choice of the SCM, thereby the prolonged or reduced open time is dependent on the type of application. For instance, a prolonged open time of a 3D printable mix may be required for large scale 3D printing.

8. Rheological properties of 3DP-CC

Rheological properties directly influence the overall printability of any mix design for 3D printing. The main rheological parameters include static yield stress, dynamic yield stress, plastic viscosity, thixotropy, structuration rate and flocculation rate. Raw cementitious material needs to have considerable amount of flowability while pumping prior to extrusion, yet low flowability and adequate thixotropy after being extruded from the nozzle to ensure better buildability [105,106]. Overall, it is important to accurately measure and analyze the rheological properties of designed materials for successful 3D printing. The rheological behaviour of cementitious composites is generally characterised by Bingham model as shown in Equation (6).

$$\tau = \tau_0 + \tau\gamma \tag{6}$$

where, τ and γ denote shear stress and shear rate, and τ_0 and μ represent yield stress and plastic viscosity, respectively [107]. For the flow of 3D printable mixtures, there are two types of stress involved: static yield stress and dynamic yield stress. Static yield stress is the minimum required stress to initiate a flow, while dynamic yield stress keeps it moving. When there is a continuous shearing force, the microstructural bond becomes weaker, causing a decrease in shear stress. In contrast, an undisturbed microstructure results in a higher static yield stress in comparison to the dynamic yield stress. As soon as the pressure is removed, the cementitious composite stops flowing, and the particles begin to re-cluster together, which brings the static yield stress back to its original level. This phenomenon is referred to as thixotropy. Thixotropic fluids are those that have a decrease in viscosity as the shear rate increases. The flow curve for a thixotropic fluid has a unique shape that forms a closed loop called a hysteresis loop curve as shown in Fig. 11.

If the "up curve" and "down curve" no longer overlap, this indicates a change in the structure of the fluid. The thixotropic performance is determined by the energy needed to disrupt or break down this structure, which is represented by the area enclosed within the loop. One way to assess the printability is by evaluating their thixotropy. The correlation between static and dynamic yield stress can aid in assessing the thixotropic performance through Equation (7) [108,109]:

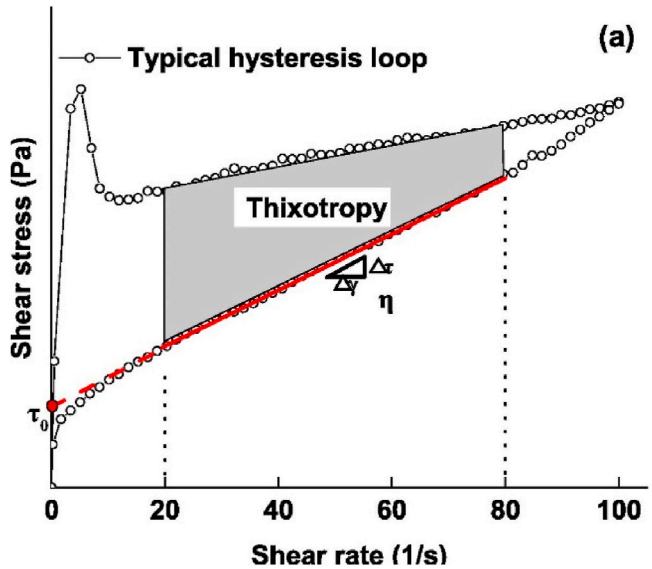

Fig. 11. Hysteresis loop curve for a thixotropic fluid [70].

$$I_{thix} = \frac{\tau_s - \tau_d}{\tau_d} \times 100\ \% \tag{7}$$

In equation (7), I_{thix} represents the thixotropic index which is a measure of thixotropy in 3D printing. In a thixotropic material, the dynamic yield stress is typically lower than the static yield stress. When the material is at rest or subjected to low shear rates, the viscosity is high, and it exhibits a solid-like behaviour due to the static yield stress being dominant. However, when the material is subjected to higher shear rates or stress, such as during mixing or pumping, the dynamic yield stress becomes dominant, causing the viscosity to decrease, and the material exhibits fluid-like behaviour and flows more easily. The difference between static and dynamic yield stress is believed to stem from thixotropy [110]. The greater the difference between the static and dynamic yield stress, the greater the thixotropy. A higher value of thixotropy index, I_{thix} indicates better thixotropy of cementitious composite.

As time passes, the static yield stress of a fresh mix rises due to the particles touching each other and the onset of cement hydration. This process is referred to as structuration [111]. The structuration rate, A_{thix} and the flocculation rate, R_{thix} are two factors that influence the thixotropy during pumping and extrusion. A_{thix} measures the increase in static yield stress over time, while R_{thix} relates to the rebuilding of the microstructure. These factors operate on different time scales, with A_{thix} acting over a longer interval due to chemical reactions, while re-flocculation occurs within a shorter time frame as shown in Fig. 12 [112]. When the print material has a high A_{thix} value, it has the ability to support its own weight through a controlled build-up rate, thereby enabling successful printing. If the print material has a low A_{thix} value, it is more likely to experience plastic collapse failure. Hence, it is crucial to choose the print material based on its A_{thix} value to ensure optimal printing conditions [113].

A_{thix}, and R_{thix} can be mathematically expressed by Equations (8) and (9) [111].

$$\tau_{s,i} = \tau_{d,i} + R_{thix}\ \ t \tag{8}$$

$$\tau_{s(t)} = \tau_{s,i} + A_{thix}\ \ \left(t - t_{rf}\right) \tag{9}$$

The equations above illustrate the static yield stress of a material at a given time t after the start of mixing, denoted as $\tau_s(t)$. The initial static yield stress of the material is represented by $\tau_{s,i}$, while the initial dynamic yield stress is denoted as $\tau_{d,i}$. Here, all the yield stress is calculated in Pa. Time since the beginning of mixing is indicated by t in seconds, while t_{rf} is the time period (in seconds) during which re-flocculation takes place and is responsible for the increase in shear stress, measured in seconds [111]. Unit of A_{thix}, and R_{thix} is Pa/s. To determine the level of thixotropy, there are two methods [114]. One is to analyze the hysteresis area of flow curves by measuring the integration of upward and downward curves. Another approach is to monitor the gradual rise in yield stress. Wangler et al. [1] introduced a way to calculate the rate of thixotropic build-up (A_{thix}) using the following Equation (10).

$$A_{thix} = \frac{\rho g h}{\sqrt{3} t_{h,min}} \tag{10}$$

where ρ, g, and h are density (kg/m^3), gravity constant (m/s^2), and layer height (m), respectively. The variable $t_{h,min}$ indicates the minimum time (in second) required for layer formation [1].

8.1. Rheological requirements for printability

To achieve successful 3D printing, it is important to maintain a balance between the rheological needs of pumping, extrusion, and buildability stages as shown in Fig. 13. This can be achieved through rheology characterization, which determines the fresh properties of the mix [115]. Zhang et al. [44] reported that three key rheological properties are vital for 3D printable mixtures. Firstly, ensuring the correct dynamic yield stress and viscosity is crucial for a proper pumping and extrusion process. Secondly, a high static yield stress is necessary to prevent deformation after extrusion. Lastly, having excellent thixotropy is desired to extend the printing process duration. These properties highly influence the overall printability condition of any mix after extrusion [105,116].

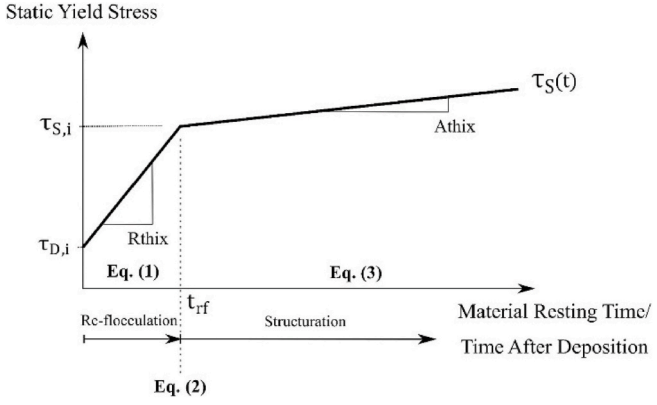

Fig. 12. Structuration rate and re-flocculation mechanism over time [111].

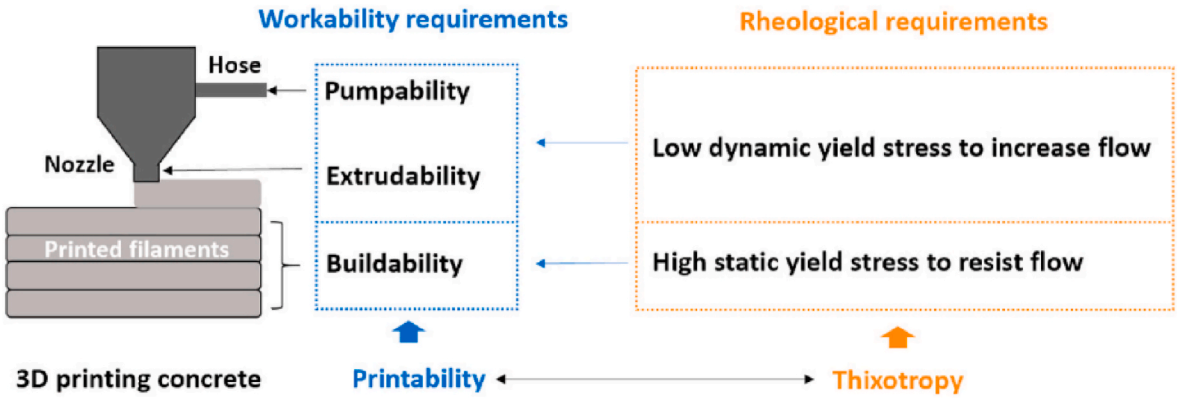

Fig. 13. Rheological requirements for 3D printing [18].

Table 7
Static yield stress values reported in previous literatures for printable mixes.

Reference	Rheometer	Static yield stress (Pa)	Binder Constituent	Fibre	Printability Condition
[76]	MCR 72 Rheometer of Anton Paar	4121.4–4221.4	OPC, WGP	–	Maximum print height 150–155 mm
[117]	MCR 101 Anton Paar®, Singapore	3200–5300	OPC, FA, SF, NC	–	Maximum print layers 10-18
[78]	Anton Paar MCR 301 Rheometer	4240	OPC, CSA, SF, FA	–	Maximum print layers 50
[118]	Viskomat XL Rheometer	3350	OPC, FA, SF	–	Maximum printed layers 42
[79]	Viskomat XL Rheometer	900–3800	OPC, SF	–	Maximum printed layers 21-320
[111]	Germann Instruments ICAR Rheometer	2730–3944	OPC, FA, SF	–	Maximum printed layers 54-59
[41]	RotoVisco RV1 Rheometer	172.1–184.1	OPC, GGBFS, CBP	–	20 layers printability with height loss of 5.9 %–6.2 %
[119]	Brookfield HD DV-III Ultra	2251.9	OPC, RHAP	–	Maximum printed layers 24
[120]	Brookfield DV-III	450	OPC, FA, SF	–	Maximum printed layers 50
[75]	Brookfield Rheometer	170–935	OPC	–	Maximum print height 262–298 mm
[121]	Rotational Rheometer (Kinexus labþ, malvern, UK)	660–730	CSA Cement, Bentonite	–	Print layer 10 (Deformation percentage 3.88 %–6.03 %)
[61]	Viskomat XL Rheometer	242–467	GP Cement, SF, NC	Steel Fibre-2% vol of binder (length 6 mm)	Maximum printed layers 7-14
[57]	Brookfield RST-SST rheometer	272.8–1131.7	OPC, FA, SAC	PE Fibre - 2 % vol of Binder (length 12 mm)	Maximum print layer 17 (vertical deformation 0.8%–4.3 %)
[80]	Shear vane apparatus	550	OPC, FA, SF	PP fibre 1.2 kg/m^3 of binder (length 12 mm)	For one-filament group, maximum 15 print layers; for five-filament group, up to 34 layers.

Note-, CBP - Crushed Brick Powder, RHASP-Rice Husk Ash Powder, CSA- Calcium Sulfoaluminate Cement, OPC- Ordinary Portland Cement, WGP-Waste Glass Powder, FA- Fly Ash, SF- Silica Fume, GGBFS- Ground Granulated Blast Furnace Slag, SAC- Sulphate Aluminate cement, PP- Polypropylene Fibre, PE- Polyethelene Fibre.

Studies have shown significant variation in rheological values among different printable mixtures for attaining optimum printability. This can be observed from Tables 7–9 which show the reported values of static yield stress, dynamic yield stress and plastic viscosity, respectively. One of the main reasons behind the large difference in corresponding values is the adoption of different types of rheometers as there lies a big difference in their results. Various types of rheometers are being referred by the existing researchers such as Viskomat XL rheometer, Anton Paar rheometer, ICAR rheometer, and Brookfield rheometer. Also, fresh 3D printable mixes are very sensitive to the chemical admixture dosage or SCM type as well as the rest time. The effects of these parameters on the rheological properties are detailed in the following sections.

Reviewing Tables 7–9 highlights significant variations in rheological values (static yield stress, dynamic yield stress, and plastic viscosity) depending on the rheometer used and the composition of the mixture. Notably, the Anton Paar rheometer, Viskomat XL rheometer, and ICAR Rheometer consistently yield higher static yield stress values (ranging from 3200 to 5300 Pa [117], 900–3800 Pa [79], and 2730–3944 Pa [111], respectively) for various 3D printable mortars. Conversely, the RotoVisco RV1 rheometer [41] and Brookfield rheometer generally provide lower rheological values of 172.1–184.1 Pa and 272.8–1131.7 Pa [57] for different mortar mixes, respectively. Similar phenomena is also observed for dynamic yield stress values. Plastic viscosity values also exhibit variations, ranging between 35 and 46 Pa s [79] computed by Viskomat XL rheometer for a 3D printable mix and 1.5–10 Pa s with other rheometers. Furthermore, the introduction of fibres into 3D printable mortars (3DP-FRCC mixes) surprisingly results in even lower static

Table 8
Dynamic yield stress values reported in printable mixes in previous literatures.

Reference	Rheometer	Dynamic yield stress (Pa)	Binder Constituent	Printability
[78]	Anton Paar MCR 301 rheometer	920	OPC, CSA, SF, FA	Maximum print layers 50
[122]	Anton Paar MCR 302 rheometer	58.6–76.2	OPC, FA, SF	Printable with 1st layer stability index of 91 %–92.5 %
[79]	Viskomat XL Rheometer	400–800	OPC, SF	Maximum printed layer 21-320
[118]	Viskomat XL Rheometer	492.7	OPC, FA, SF	Maximum printed layers 42
[111]	Germann Instruments ICAR Rheometer	1146–1532	OPC, FA, SF	Maximum printed layers 54
[41]	RotoVisco RV1 Rheometer	27–29.4	OPC, GGBFS, CBP	20 layers printability with height loss of 5.9 %–6.2 %
[121]	Rotational Rheometer (Kinexus labþ, malvern, UK)	300–700	CSA Cement, Bentonite	Print layer 10 (Deformation percentage 3.88 %–6.03 %)

Note-, CBP - Crushed Brick Powder, CSA- Calcium Sulfoaluminate Cement, OPC- Ordinary Portland Cement, WGP-Waste Glass Powder, FA- Fly Ash, SF- Silica Fume, GGBFS- Ground Granulated Blast Furnace Slag.

Table 9
Plastic viscosity values for printable mixtures reported in previous literatures.

Reference	Rheometer	Plastic viscosity (Pa.s)	Binder Constituent	Fibre	Printability
[121]	Rotational Rheometer (Kinexus labþ, malvern, UK)	2.5–3	CSA Cement, Bentonite	–	Print layer 10 (Deformation percentage 3.88 %–6.03 %)
[122]	Anton Paar MCR 302 rheometer	1.7–4	OPC, FA, SF	–	Printable with 1st layer stability index of 91 %–92.5 %
[123]	Dynamic shear rheometer (TA instruments AR2000EX)	4.35	OPC, LF	–	Buildable and Extrudable
[79]	Viskomat XL Rheometer	35–46	OPC, SF	–	Maximum printed layer 21-320
[118]	Viskomat XL Rheometer	16.65	OPC, FA, SF	–	Maximum printed layers 42
[95]	Viscomter 5 Rheometer from ConTec Iceland	10.1	OPC, SF	Basalt Fibre- 0.003 vol of binder (9 mm length)	Uniform and accurate extrudability for 20 mm strip print filament
[120]	Brookfield DV-III	21	OPC, FA, SF	–	Maximum printed layers 50

Note- CBP - Crushed Brick Powder, CSA- Calcium Sulfoaluminate Cement, OPC- Ordinary Portland Cement, WGP-Waste Glass Powder, FA- Fly Ash, SF- Silica Fume, LF-Limestone Filler, GGBFS- Ground Granulated Blast Furnace Slag.

yield stress values (242–467 Pa with Viskomat rheometer [61] and 272.8–1131.7 Pa with Brookfield RST-SST rheometer [57]) compared to mortars without fibres. This contradicts the theoretical expectation and warrants further investigation into the effects of fibre inclusion on rheological properties in 3D printable mixes. These variations may stem from different rheometers used, testing at various rest times, differences in chemical admixture dosage, and the use of different SCM with varying dosages. To enhance consistency, it is recommended to standardize measurement methods across all rheometers and conduct rheological tests with uniform rest times and detailed mix constituent specifications.

8.2. Effect of superplasticizer on rheology

SP increases the fluidity of 3D printable cementitious materials by reducing the attractive forces between cement particles and simultaneously decreasing yield stress and plastic viscosity. Various types of SP have different levels of effectiveness. Among melamine resin-based, modified lignosulphonate-based, and modified polyacrylate-based SP, the modified polyacrylic SP was found to be the most effective in enhancing the rheological properties of cement paste. Naphthalene SP helps to disperse cement while avoiding air entrainment and slump retention effects [40]. Le et al. [80] found that application of 1–1.5 % polycarboxylate polymer based SP in mortar resulted in shear strength values of 0.3–0.9 kPa, which was reported to exhibit good extrudability. Polycarboxylate SP, made up of a polyethylene backbone and PEO-grafted chains with carboxylic groups, disperses cement particles, reduces slump loss, and speeds up the setting time. It has also been reported that liquid polycarboxylate was observed to be more effective than solid polycarboxylate based SP [40]. Rahul et al. [93] found that the ideal yield stress value for good buildability was 1600 Pa when using a 0.1 % SP dosage. Dosages lower than this were not sufficient for successful extrusion, while higher dosages made it challenging to build printed structures. According to Xiao et al. [59], adding 0.13 % SP (by weight of the binders) improved the pumpability of 3D printable mix.

8.3. Effect of VMA on rheology

VMA are new additives that improve the rheology of cementitious composites by increasing its consistency and cohesiveness. Unlike SP, VMA improves the yield stress and buildability performance while sacrificing flowability and pumpability performances [124]. The numerous hydrogen bonds in VMA such as HPMC molecules facilitate adsorption onto material surfaces and hydration products, physically bridging them together, resulting in increased yield stress and thixotropy at an early stage. According to Schmidt

et al. [125], VMA has a more significant impact on yield stress than polycarboxylate ether superplasticizer at 20 °C. Although SP increases flowability, it may not entirely prevent issues like segregation and bleeding. In such cases, adding HPMC can enhance stability, cohesion, and mitigate water evaporation and drying shrinkage. The function of VMAs is to adsorb and bridge cement particles, thereby increasing the yield stress [37].

Yun et al. [126] found that using HPMC based VMA tended to decrease flow resistance and increase torque viscosity, negatively affecting pumpability. HPMC also thickens the viscosity of free water improving overall mortar's viscosity. Additionally, HPMC delays the early-stage hydration process, enhancing the printability of 3D printable cementitious mixtures. Even after a 30-min standing time, HPMC significantly amplifies yield stress and viscosity, exceeding the natural increase in rheological properties [59]. By adding small amounts of HPMC (0.01 %, 0.03 %, and 0.05 % of the cement's mass), the printability of the mortar was reported to be significantly improved [59]. Kilic et al. [78] found that with the addition of VMA, static yield stress and dynamic yield stress as well as plastic viscosity got increased. Similarly, Yin et al. [77] also reported a significant improvement in rheological properties due to the inclusion of HPMC. Without HPMC, the mix had significantly lower yield stress, making it difficult to achieve the desired results. For instance, when 0.2 % HPMC was added to the mix, the static yield stress values increased to approximately 685 Pa, 807 Pa, 1100 Pa, 1464 Pa, and 2160 Pa at 5, 20-, 35-, 50-, and 65-min hydration times, respectively. On the other hand, the corresponding values for the reference mix without HPMC were only 201 Pa, 196 Pa, 220 Pa, 382 Pa, and 752 Pa, which were significantly lower than those of the mix with HPMC. The improvement was further attributed to three key factors. Firstly, it enhanced the initial static and dynamic yield stress, which helped maintain the size of the mortar after leaving the extrusion barrel, improving its extrudability and buildability. Secondly, within a certain range, the increased dynamic yield stress allowed the mortar to flow against gravity, ensuring it remained in the extrusion barrel and improving its pumpability. Thirdly, HPMC delayed the hydration process and reduced the acceleration rate of yield stress, which extended the open time of the mortar and led to increased mortar cohesion and improved thixotropy.

In general, it can be inferred that the incorporation of HPMC significantly affects buildability and extrudability performance for preparing 3D printable mixes. However, if the VMA dosage is too high, in that case, it may worsen the mix by making it difficult to pump out by pipelines due to the higher energy required for the stiffer mix. Therefore, a proper optimization of VMA dosage is very necessary for every individual mix to get the desired printability performance. It should also be noted that the type of VMA may also affect the performance. For instance, Leemann et al. [127] demonstrated that VMA based on polysaccharide caused the largest increase in yield stress, while VMA based on microsilica resulted in the lowest yield stress for an equivalent plastic viscosity.

8.4. Effect of retarder on rheology

Retarding admixtures are employed to slow down the setting rate of cementitious composites and offset the accelerated effect of setting. These additives help keep concrete workable for a longer period and delay its initial setting by slowing down the structurization rate (A_{thix}). This results in a longer open time, allowing for continuous 3D printing for large-scale construction projects. Souza et al. [83] reported that a commercially available setting retarder (CSR) was more efficient than sucrose in lowering yield stress. The optimum contents of CSR and sucrose were found respectively 0.1 % and 0.05 % by weight of binder. Within the initial 30 min of hydration, A_{thix} experienced a decrease of roughly 50 % when accompanied by a CSR of up to 0.1 %. However, when sucrose was used at an optimized concentration of 0.05 %, the reduction in A_{thix} was approximately 20 %. Ahmad et al. [128] conducted a similar study and discovered that the addition of sugar as a setting retarder had an optimal retarding effect at 0.05 %. In a study conducted by Zou et al. [75], various dosage of sodium gluconate (0 %, 1.2 %, and 1.6 % of binder weight) were tested as retarders for 3D printable mix designs that used recycled fine aggregate instead of river sand. It was reported that the addition of sodium gluconate had a negative impact on the buildability performance. However, the researchers found that incorporating recycled fine aggregate (50 %, 100 %) had positive effects on certain properties, including increase of yield stress, viscosity, and thixotropic loop area. The study revealed that the best printing results were achieved by using a mix of 100 % recycled fine aggregate and 1.2 % sodium gluconate, leading to 20 layers of printing.

8.5. Effect of fibres on rheology

Generally, flowability decreases and buildability increases with the increase in fibre dosage. In rheological perspective, addition of fibres increases the yield stress and plastic viscosity which improves the buildability, whereas sacrifices the pumpability performance. Arunothayan et al. [61] investigated the rheological properties of ultra-high performance fibre-reinforced composites with a focus on the effects of the volume of steel fibres (0 %, 1 %, and 2 %) and the mass of NC (0 %, 0.1 %, and 0.2 % relative to the binder) on flowability, static yield stress, dynamic yield stress, apparent viscosity, extrudability, and buildability of the printed mixtures. The results showed that the mixtures with a higher dosage of steel fibres exhibited a higher static yield stress at all resting times. For instance, at 5 min of rest time, the static yield stress of mixtures with 0 %, 1 %, and 2 % steel fibres were 65 Pa, 69 Pa, and 322 Pa, respectively. The inclusion of steel fibres also resulted in an increase in dynamic yield stress, apparent viscosity, and shear-thinning behaviour. The rise in yield stress due to the addition of steel fibres can be attributed to the rigidity of the fibres, which enhanced the composite's yield stress. Tran et al. [129] studied the rheological impact of incorporating PP fibres into a 3D printable cementitious mixture. The research revealed that adding PP fibres, ranging from 1.35 to 5.4 kg/m^3 of the cementitious mix, resulted in a substantial increase in both plastic viscosity and dynamic yield stress values, with approximately 400 % and 320 % increases, respectively. Similar results were found by Weng et al. [97] where they used 8 mm length PVA fibre with 1.2 % oil coating and found that increasing the amount of fibres increased the flow resistance, torque viscosity and thixotropy.

8.6. Effect of different SCM on rheology

Different SCM have different types of effect on rheology of fresh mix. Among different SCMs, SF incorporation was found to be a

desirable ingredient for 3D printable mortars, and it is identified as a suitable ingredient for adjusting the rheological properties of 3D printable cementitious materials. Mechtcherine et al. [130] discovered that the inclusion of SF along with additional water not only enriches the fines content in the mixture but also reduces the plastic viscosity. This dual effect ultimately enhances the pumpability of conventional mixes. On a similar note, Choi et al. [131] observed that the proportion of SF in comparison to other SCMs like GGBFS and FA notably influences the thickness of the lubricating layer. This is likely due to the relatively finer particle size of SF. Their study demonstrated that a mixture containing a 5 % replacement of OPC with SF led to a significant improvement in the efficiency of pumping operations by reducing plastic viscosity.

Xu et al. [89] aimed to create a 3D printable cement-based mortar using FA and GGBFS as SCM at 0–40 % replacement ratio. They observed that the pastes exhibited optimal apparent viscosity, and shear stress at 20 % FA, resulting in improved extrusion and buildability. The addition of FA improved fluidity due to its ball bearing effect and filling of spaces between cement particles. The fineness of FA particles also enhanced the particle gradation and homogeneity of the cement paste. Adding GGBFS to the mix also increased particle size distribution and minimized friction between paste particles, resulting in improved rheological characteristics of the mortar. However, utilization of excessive GGBFS caused a significant rise in the water demand and unfavourable paste viscosity. Overall, the research found that the addition of FA and GGBFS can enhance the rheological properties of the slurry, especially when the content is at 20 %. Weng et al. [97] and Varela et al. [90] also reported that incorporation of FA increased torque viscosity, while decreasing the thixotropy. Yu et al. [155] further studied the impact of varying GGBFS dosages on the rheological properties of mortar-based composites. When the GGBFS content was increased from 0 % to 10 %, the static yield stress value rose from 6795.2 Pa to 6981.7 Pa. However, as the GGBFS percentage was further increased to 20 %, 30 %, 40 %, and 50 %, the static yield stress values saw a significant reduction, dropping to 5641.1 Pa, 5340.4 Pa, 4635.1 Pa, and 4290.6 Pa, respectively. Similarly, dynamic yield stress and plastic viscosity showed an initial increase with the addition of GGBFS from 0 % to 10 %, followed by a decrease with higher replacement percentages. Specifically, dynamic yield stress increased from 209.4 Pa to 216.2 Pa within the 0 %–10 % range, but then decreased to 146.9 Pa with 50 % GGBFS. In terms of thixotropy, an increase in GGBFS percentage led to a reduction in the thixotropic index, with values decreasing to 31.2, 28.6, 23.4, 16.6, 15.2, and 13.9 kPa/s for 0 %, 10 %, 20 %, 30 %, 40 %, and 50 % GGBFS, respectively.

Researchers have also evaluated the effect of other SCMs such as rice husk ash (RHA), NC, LF, MK on the rheological properties of 3DP-CC, however, the research is very limited. Tinoco et al. [119] conducted a study to explore the effects of replacing OPC with RHA on the rheology of mortar. Replacing 5 %–15 % OPC with dry RHA increased static yield stress from 367.7 Pa to 2251.9 Pa, dynamic yield stress from 142.3 Pa to 943.3 Pa, plastic viscosity from 5.09 Pa s to 7.94 Pa s, and structuration rate from 8.84 Pa/min to 23.4 Pa/min. A study conducted by Lopez et al. [132] examined the influence of LF and MK on the rheological properties. They found that LF decreased the yield stress and plastic viscosity by reducing the number of flocculated cement particles. On the other hand, MK added to ternary binders offset this effect by enhancing rheological parameters due to its high specific surface area. Arunothayan et al. [61] reported that incorporating NC into 3D printable mixes has a significant impact on their rheological characteristics. The results showed that higher levels of NC led to increases in static yield stress, dynamic yield stress, apparent viscosity, flocculation rate, and thixotropy. In mixes without fibres, the yield stress increased to 65 Pa, 205 Pa, and 242 Pa for 0 %, 0.1 %, and 0.2 % NC addition, respectively. Similarly, the thixotropic index increased to 15, 50, and 63. They suggested that the increase in static yield stress could be attributed to the formation of a lattice microstructure that suspended solid particles in the fresh mixture, resulting in a higher flocculation rate and static yield stresses.

8.7. *Effect of superabsorbent polymers (SAP) on rheology*

SAP are hydrophilic polymer networks that have the ability to absorb an exceptionally large amount of water or aqueous solutions. The inclusion of SAP serves as a safeguard that prevents excessive shrinkage, while also promoting freeze-thaw resistance.

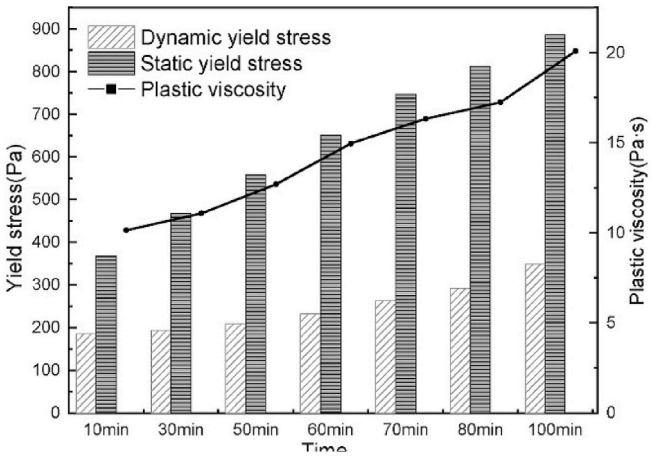

Fig. 14. Effect of rest time on rheological values [95].

Furthermore, it provides the material with self-healing properties [133]. These characteristics make it a desirable feature for 3D printable materials. According to Liu et al. [134], the inclusion of SAP can increase the yield stress by up to 4 times. Secrieru et al. [135] also reported an increase in the plastic viscosity and yield stress of cement-based composites by the addition of SAP. Oh et al. [133] studied the rheological behaviour of cement mortar with varying SAP dosages, particle sizes, and superplasticizer presence. The impact of SAP on rheological properties was significant, as it promoted structuration in mixtures without SP, but reversed the effect in mixtures with SP and a low water-cement ratio. In addition, Ma et al. [136] also observed that adding large particle SAP increased the yield stress and plastic viscosity of low water-to-binder ratio cement-based materials.

8.8. Effect of rest time on rheology

In 3D printing, the standing time which is also referred as rest time has a significant impact of the prepared 3D printable cementitious composites. With the increase of rest time after water addition of mix, the static yield stress, dynamic yield stress, plastic viscosity increases due to increased structurization rate and hydration process. However, if the standing time is too long, the material may become difficult to pump and extrude out due to increased viscosity and reduced workability. Therefore, finding the right balance between standing time and printability is crucial. Xiao et al. [59] conducted a rheological based study for 3D printable mortar and investigated the effects of standing time (15 min, 30 min, and 45 min) on the rheological properties of mortar. The results showed that as the standing time increased, the loss of flowability also increased by around 5 %, 8.5 %, and 11 % respectively. For dynamic yield stress, the increase was around 112 %, 165 %, and 396 % respectively. For static yield stress, the increase was 10.5 %, 29 %, and 90 % respectively. Moreover, the plastic viscosity of the mortar increased by around 4.5 %, 29.5 %, and 32 % respectively. This increase was due to the flocculation and hydration of binders. As the standing time increased, the interaction force and net structure of the mortar became stronger, leading to an increase in plastic viscosity [59]. In a study conducted by Deng et al. [76], WGP was incorporated as SCM at different concentrations (0 %, 20 %, 40 %, and 60 %) of the binder weight. It was observed that with the increase in rest time from 0 min to 30 min, 60 min, and 90 min, both static and dynamic yield stress values increased for all the investigated mixtures. The mixture containing 40 % WGP showed a static yield stress value of 4147 Pa at just after mix preparation, which increased to 9164 Pa at 90 min of rest time, with an average increasing rate of 23 Pa/min. However, for dynamic yield stress, the increasing rate was noted to be 30 Pa/min. The rise in both static and dynamic yield stress was attributed to the higher hydration level with the passage of rest time for the investigated mixtures. Zhao et al. [95] showed that the rheological values increased as the rest time increased from 10 min to 100 min as shown in Fig. 14. For instance, the static yield stress increased from 367.4 Pa to 886.2 Pa (141 % increase), while dynamic yield stress values increased from 185.8 Pa to 348.9 Pa (87 % increase). Similarly, plastic viscosity values increased by 99 % from 10.1 Pa to 20.1 Pa. Therefore, optimizing the correct rest time for printing is compulsory for getting the best printing performance. As the rheological values increase with rest time, they may exceed the suitable values for the corresponding 3D printing machine, making it lose its pumpability and extrudability.

9. Summary and conclusions

9.1. Summary

The 3DP-CC emerges as the future of the construction industry, marking a remarkable advancement in digitalized and innovative construction technology. However, this transformative technology is still in its early stages, necessitating further in-depth exploration. This comprehensive review paper extensively explores the research on fresh property parameters and rheological properties in both 3DP-CC and 3DP-FRCC. Furthermore, it thoroughly analyses the impact of mix constituents such as SCM, SP, VMA, fibres, sand-to-binder ratio, and water-to-binder ratio on each fresh property parameter and rheological aspect. Based on the critical review, the following conclusions are drawn.

- Flowability is greatly affected by the composition of the mixture. SCM such as FA, GGBFS, and LF enhance flowability, while SF and NC have the opposite effect. SP improves flowability, but VMA counteracts it. The addition of fibres significantly reduces flowability. To achieve optimum printability performance, it is recommended to keep the flowability range within 160–200 mm by adjusting chemical admixtures and other mix constituents.
- Buildability can be estimated using any of the three test methods namely indirect buildability test by imposing weight, layer deformation method and maximum print layer or layer height count method. Among these, the indirect buildability test enables to determination of the buildability without using 3D printing machine, whereas other two methods require 3D printing machine.
- Buildability of a mix can be enhanced by incorporating NC, SF, MK as SCM. Adding fibre and VMA also enhances buildability by reducing segregation of mix constituents. However, addition of LF and SP may reduce buildability performance.
- Extrudability test is generally conducted by visual observation of the uninterrupted length and thickness of the filament by printing directly with 3D printing machine or by ram extruder. The extrudability of a 3D printable mix can be improved using FA, GGBFS, NC, SP, and VMA. However, addition of fibre requires adjustment of SP and VMA to obtain desired extrudability.
- Rheology of a 3D printable mix is highly sensitive to the study type. For proper attainment of printability performance, mix constituents especially chemical admixtures including SP, VMA, retarder, SAP should be optimized very carefully. Overdosing or inadequate dosage of any of the chemical admixtures may drastically affect the rheological properties resulting in failure of overall printing process.
- The use of SF has been found to be helpful in reducing plastic viscosity, enhancing pumpability performance, and extending the open time of a 3D printable mix. However, it is important to properly optimize the SP and VMA for optimal pumpability

performance, especially when adding fibre to the mix. Fibres generally cause the mix to become stiff and cohesive, making the pumpability process difficult. NC addition is also recommended to improve static yield stress as it is very effective even at low dosage.

- Rheological test results are also highly dependable upon rheometer used, mix ingredients and time of testing after water addition. Similar mix design can exhibit high variation of rheological test results depending on the type of rheometer used, variation on mix ingredients and on rest time. The Anton Paar rheometer, Viskomat XL rheometer, and ICAR Rheometer consistently yield higher static yield stress values (ranging from 3200 to 5300 Pa, 900–3800 Pa, and 2730–3944 Pa respectively for various 3D printable mortars. Conversely, the RotoVisco RV1 rheometer and Brookfield rheometer generally provide lower rheological values of 172.1–184.1 Pa and 272.8–1131.7 Pa for different mortar mixes respectively.
- The selection of mix constituents, such as FA, GGBFS, and SF, is crucial in determining the overall rheological properties of a 3D printable mix. These SCM can enhance the rheological properties up to a certain level of binder replacement percentage for each type of SCM. However, beyond that percentage, the rheological properties may exhibit contrasting effects.
- Based on the reported observations, a generalised effect of different mix constituents on fresh and rheological properties can be summarized in Table 10.

9.2. *Recommendations for future research*

Some potential future research recommendations related with 3DP-CC and 3DP-FRCC are described below.

- There is a clear lack of building-code systems for 3D printing processes, encompassing design standards, calculation methods, and construction techniques. Subsequent research efforts should prioritize the formulation of design philosophies and standards tailored specifically to 3D printable composites, especially recommendation of optimum range of the fundamental design parameters.
- The sensitivity of rheological test outcomes to equipment variations has led to fluctuations in the optimized result ranges reported in previous literature. It is crucial to address these inconsistencies by establishing standardized test methods, ensuring a consistent interpretation of rheological test results across diverse research environments.
- Optimum result ranges considering all types of composites including, mortar, fibre reinforced cementitious composites and ordinary concrete, should be standardized with respect to fresh property as well as rheological aspects which can be a benchmark for future researchers to prepare any novel 3D printable cementitious composites. This will also require a simultaneous analysis of the mechanical property aspects, and anisotropic effects in 3D-printed specimens. Detailed numerical simulations can further help in generalising these parameters on which many studies exist but are not covered in this paper.
- Flowability test is more practical for on-site application in comparison to rheological tests. Therefore, detailed studies need to be conducted to establish a correlation between fresh property tests and corresponding rheological test results for different types of cementitious composites and high-performance concrete.
- The pumpability and open time properties are least experimented among all other fresh property parameters. For large construction works, pumpability holds significant importance, and it can be affected by factors such as varying pipe lengths, pipe diameter, temperature, rheological changes post-pumping, and the influence of pumping unit power. Therefore, additional comprehensive research is required to better understand these aspects.
- Though the volume and type of fibres such as PP, PVA, PE have shown clear impact on both fresh properties and rheological parameters, the research on 3DP-FRCC is at a very early stage and further investigation is necessary to understand the characteristics of 3DP-FRCC with different types of fibres. Additionally, there is a growing interest on the use of natural fibres in recent years. However, due to limited research, these type of fibres were not covered in this paper and may be explored in future studies.

CRediT authorship contribution statement

Mahfuzur Rahman: Writing – original draft, Visualization, Investigation, Formal analysis, Data curation, Conceptualization. **S.**

Table 10
Summary of effects of mix constituents on fresh and rheological properties.

Mix Constituent	Fresh Properties					Rheological Properties		
	Flowability	Buildability	Extrudability	Pumpability	Open time	Static yield Stress	Dynamic yield stress	Plastic viscocity
Fly ash	↑	–	↑	↑	↑	↓	↓	↓
Ground granulated blast furnace slag	↑	–	↑	↑	↓	↓	↓	↓
Limestone filler	↑	↓	–	–	↑	↓	–	↓
Metakaolin	↓	↑	–	–	↓	↑	–	↑
Silica fume	↓	↑	–	↑	↑	–	↓	↓
Nano clay	↓	↑	↑	↓	↓	↑	↑	↑
SP (Polycarboxylate Ether)	↑	↓	↑	↑	↑	↓	↓	↓
VMA (Hydroxypropyl Methylcellulose)	↓	↑	↑	↑	↑	↑	↑	↑
Fibre (Metal and Polymer)	↓	↑	↑	↑	↓	↑	↑	↑

Here, ↑ indicates that the respective parameter value generally shows an increasing trend with the addition of the constituent, whereas ↓ the opposite.

Rawat: Writing – review & editing, Validation, Supervision, Methodology, Conceptualization. **Richard (Chunhui) Yang:** Writing – review & editing, Supervision, Resources. **Ahmed Mahil:** Writing – review & editing, Supervision. **Y.X. Zhang:** Writing – review & editing, Supervision, Resources, Project administration, Funding acquisition, Conceptualization.

Declaration of competing interest

The authors declare that they have no known competing financial interests or personal relationships that could have appeared to influence the work reported in this paper.

Data availability

Data will be made available on request.

References

[1] T. Wangler, et al., Digital concrete: a review, Cement Concr. Res. 123 (2019) 105780.
[2] A.C.C.M.-. Standard Test Method for Compressive Strength of Cylindrical Concrete Specimens, ASTM International, West Conshohocken, PA, 2021.
[3] S.C. Paul, et al., Fresh and hardened properties of 3D printable cementitious materials for building and construction, Arch. Civ. Mech. Eng. 18 (2018) 311–319.
[4] B.B. Jindal, P. Jangra, 3D Printed Concrete: a comprehensive review of raw material's properties, synthesis, performance, and potential field applications, Construct. Build. Mater. 387 (2023) 131614.
[5] E. Booya, et al., The performance of slag containing engineered cementitious composites, in: IOP Conference Series: Materials Science and Engineering, IOP Publishing, 2020.
[6] S. Lim, et al., Developments in construction-scale additive manufacturing processes, Autom. ConStruct. 21 (2012) 262–268.
[7] J. Malda, et al., 25th anniversary article: engineering hydrogels for biofabrication, Adv. Mater. 25 (36) (2013) 5011–5028.
[8] S.V. Murphy, A. Atala, 3D bioprinting of tissues and organs, Nat. Biotechnol. 32 (8) (2014) 773–785.
[9] V. Markin, et al., 3D-printing with foam concrete: from material design and testing to application and sustainability, J. Build. Eng. 43 (2021) 102870.
[10] S. Bhattacherjee, et al., Sustainable materials for 3D concrete printing, Cement Concr. Compos. 122 (2021) 104156.
[11] A. Curth, 3-D Printed Concrete, Structure Magazine, July, 2022. Assessed: May, 2024 [Online] Available at : https://www.structuremag.org/?p=20944.
[12] V. Montjoy, Infographic: the Evolution of 3D Printing in Architecture, since 1939, 2023 [cited 2024 04 jan 2024].
[13] S. Nehme, A. Abeidi, 3D concrete printing, Epitoanyag-Journal of Silicate Based & Composite Materials 74 (5) (2022).
[14] F. Ceccanti, et al., 3D printing technology for a moon outpost exploiting lunar soil, in: Proceeding of the 61st International Astronautical Congress IAC, 2010.
[15] J.H. Lucas Carolo, 3D Printed House: 25 Most Important Projects, 2022.
[16] P. Hanaphy, US Marines Use Icon 3D Printing to Create Concrete Structures at Camp Pendleton, 2021.
[17] J. Teixeira, et al., Influence of supplementary cementitious materials on fresh properties of 3D printable materials, Sustainability 14 (2022) 3970, 2022, s Note: MDPI stays neutral with regard to jurisdictional claims in published ….
[18] C. Zhang, et al., Mix design concepts for 3D printable concrete: a review, Cement Concr. Compos. 122 (2021) 104155.
[19] T.K.N. Quah, et al., Concrete 3D printing: process parameters for process control, monitoring and diagnosis in automation and construction, Mathematics 11 (6) (2023) 1499.
[20] Y. Zhou, et al., Enhancement of 3D printed cementitious composite by short fibers: a review, Construct. Build. Mater. 362 (2023) 129763.
[21] A. Ramezani, et al., Effects of different types of fibers on fresh and hardened properties of cement and geopolymer-based 3D printed mixtures: a review, Buildings 13 (4) (2023) 945.
[22] G.H. Ahmed, N.H. Askandar, G.B. Jumaa, A review of largescale 3DCP: material characteristics, mix design, printing process, and reinforcement strategies, in: Structures, Elsevier, 2022.
[23] S.K. Kaliyavaradhan, et al., Test methods for 3D printable concrete, Autom. ConStruct. 142 (2022) 104529.
[24] M.K. Mohan, et al., Extrusion-based concrete 3D printing from a material perspective: a state-of-the-art review, Cement Concr. Compos. 115 (2021) 103855.
[25] V.C. Li, et al., On the emergence of 3D printable engineered, strain hardening cementitious composites (ECC/SHCC), Cement Concr. Res. 132 (2020) 106038.
[26] N. Singh, F. Colangelo, I. Farina, Sustainable non-conventional concrete 3D printing—a review, Sustainability 15 (13) (2023) 10121.
[27] Z. Zhao, et al., A critical review on reducing the environmental impact of 3D printing concrete: material preparation, construction process and structure level, Construct. Build. Mater. 409 (2023) 133887.
[28] S. Paritala, et al., Rheology and pumpability of mix suitable for extrusion-based concrete 3D printing–A review, Construct. Build. Mater. 402 (2023) 132962.
[29] D. Jiao, et al., Thixotropic structural build-up of cement-based materials: a state-of-the-art review, Cement Concr. Compos. 122 (2021) 104152.
[30] S.C. Paul, et al., A review of 3D concrete printing systems and materials properties: current status and future research prospects, Rapid Prototyp. J. 24 (2018) 784–798.
[31] Y.W.D. Tay, Y. Qian, M.J. Tan, Printability region for 3D concrete printing using slump and slump flow test, Compos. B Eng. 174 (2019) 106968.
[32] G. Ma, Z. Li, L. Wang, Printable properties of cementitious material containing copper tailings for extrusion based 3D printing, Construct. Build. Mater. 162 (2018) 613–627.
[33] K. Yu, et al., 3D-printable engineered cementitious composites (3DP-ECC): fresh and hardened properties, Cement Concr. Res. 143 (2021) 106388.
[34] C1437, A, Standard Test Method for Flow of Hydraulic Cement Mortar, 1999.
[35] Z.T. Yao, et al., A comprehensive review on the applications of coal fly ash, Earth Sci. Rev. 141 (2015) 105–121.
[36] A. Beycioğlu, H.Y. Aruntaş, Workability and mechanical properties of self-compacting concretes containing LLFA, GBFS and MC, Construct. Build. Mater. 73 (2014) 626–635.
[37] M. Jalal, M. Fathi, M. Farzad, RETRACTED: Effects of Fly Ash and TiO2 Nanoparticles on Rheological, Mechanical, Microstructural and Thermal Properties of High Strength Self Compacting Concrete, Elsevier, 2013.
[38] A. Bakhshi, R. Sedghi, M. Hojati, A preliminary study on the mix design of 3D-printable engineered cementitious composite, in: Tran-SET 2021, American Society of Civil Engineers Reston, VA, 2021, pp. 199–211.
[39] C.F. Ferraris, K.H. Obla, R. Hill, The influence of mineral admixtures on the rheology of cement paste and concrete, Cement Concr. Res. 31 (2) (2001) 245–255.
[40] D. Jiao, et al., Effect of constituents on rheological properties of fresh concrete-A review, Cement Concr. Compos. 83 (2017) 146–159.
[41] Y. Zhao, et al., Development of low-carbon materials from GGBS and clay brick powder for 3D concrete printing, Construct. Build. Mater. 383 (2023) 131232.
[42] P. Ganesh, A.R. Murthy, Tensile behaviour and durability aspects of sustainable ultra-high performance concrete incorporated with GGBS as cementitious material, Construct. Build. Mater. 197 (2019) 667–680.
[43] H.M. Hamada, et al., Effect of silica fume on the properties of sustainable cement concrete, J. Mater. Res. Technol. 24 (2023) 8887–8908.
[44] Y. Zhang, et al., Fresh properties of a novel 3D printing concrete ink, Construct. Build. Mater. 174 (2018) 263–271.
[45] R.A. Mahmood, N.U. Kockal, Effects of silica fume and micro silica on the properties of mortars containing waste PVC plastic fibers, Microplastics 1 (4) (2022) 587–609.
[46] A. Habibi, et al., RSM-based evaluation of mechanical and durability properties of recycled aggregate concrete containing GGBFS and silica fume, Construct. Build. Mater. 270 (2021) 121431.

[47] D. Wang, et al., A review on use of limestone powder in cement-based materials: mechanism, hydration and microstructures, Construct. Build. Mater. 181 (2018) 659–672.
[48] M.S. Barbosa, et al., Development of composites for 3D printing with reduced cement consumption, Construct. Build. Mater. 341 (2022) 127775.
[49] J. Teixeira, et al., Influence of supplementary cementitious materials on fresh properties of 3D printable materials, Sustainability 14 (7) (2022) 3970.
[50] J. Camiletti, A. Soliman, M. Nehdi, Effects of nano-and micro-limestone addition on early-age properties of ultra-high-performance concrete, Mater. Struct. 46 (2013) 881–898.
[51] K. Farhan, W. Gul, Impact of metakaolin on cement mortar and concrete: a review, Int. J. Civ. Eng. Technol. 8 (4) (2017) 2157–2172.
[52] R. Homayoonmehr, A.A. Ramezanianpour, M. Mirdarsoltany, Influence of metakaolin on fresh properties, mechanical properties and corrosion resistance of concrete and its sustainability issues: a review, J. Build. Eng. 44 (2021) 103011.
[53] Y. Zhang, F. Aslani, Development of fibre reinforced engineered cementitious composite using polyvinyl alcohol fibre and activated carbon powder for 3D concrete printing, Construct. Build. Mater. 303 (2021) 124453.
[54] X. Sun, et al., PVA fibre reinforced high-strength cementitious composite for 3D printing: mechanical properties and durability, Addit. Manuf. 49 (2022) 102500.
[55] F. Aslani, et al., Mechanical and shrinkage performance of 3D-printed rubberised engineered cementitious composites, Construct. Build. Mater. 339 (2022) 127665.
[56] H. Ogura, V.N. Nerella, V. Mechtcherine, Developing and testing of strain-hardening cement-based composites (SHCC) in the context of 3D-printing, Materials 11 (8) (2018) 1375.
[57] B. Zhu, et al., Development of 3D printable engineered cementitious composites with ultra-high tensile ductility for digital construction, Mater. Des. 181 (2019) 108088.
[58] J. Ye, et al., Effect of polyethylene fiber content on workability and mechanical-anisotropic properties of 3D printed ultra-high ductile concrete, Construct. Build. Mater. 281 (2021) 122586.
[59] M. Bai, et al., Workability and hardened properties of 3D printed engineered cementitious composites incorporating recycled sand and PE fibers, J. Build. Eng. (2023) 106477.
[60] A. Singh, et al., Mechanical and macrostructural properties of 3D printed concrete dosed with steel fibers under different loading direction, Construct. Build. Mater. 323 (2022) 126616.
[61] A.R. Arunothayan, et al., Rheological characterization of ultra-high performance concrete for 3D printing, Cement Concr. Compos. 136 (2023) 104854.
[62] Y. Yang, et al., Mechanical anisotropy of ultra-high performance fibre-reinforced concrete for 3D printing, Cement Concr. Compos. 125 (2022) 104310.
[63] L. Li, et al., Feasibility of glass/basalt fiber reinforced seawater coral sand mortar for 3D printing, Addit. Manuf. 37 (2021) 101684.
[64] S. Chu, L. Li, A. Kwan, Development of extrudable high strength fiber reinforced concrete incorporating nano calcium carbonate, Addit. Manuf. 37 (2021) 101617.
[65] M. Bohuchval, et al., Rheological properties of 3D printing concrete containing sisal fibres, Academic Journal of Civil Engineering 37 (2) (2019) 249–255.
[66] A. Kwan, W. Fung, Effects of SP on flowability and cohesiveness of cement-sand mortar, Construct. Build. Mater. 48 (2013) 1050–1057.
[67] W. Zhou, et al., Influence of printing parameters on 3D printing engineered cementitious composites (3DP-ECC), Cement Concr. Compos. 130 (2022) 104562.
[68] Z. Li, L. Wang, G. Ma, Method for the enhancement of buildability and bending resistance of 3D printable tailing mortar, International Journal of Concrete Structures and Materials 12 (1) (2018) 1–12.
[69] S. Hou, et al., Fresh properties of 3D printed mortar with recycled powder, Construct. Build. Mater. 309 (2021) 125186.
[70] Y. Zhang, et al., Rheological and harden properties of the high-thixotropy 3D printing concrete, Construct. Build. Mater. 201 (2019) 278–285.
[71] M. Papachristoforou, V. Mitsopoulos, M. Stefanidou, Evaluation of workability parameters in 3D printing concrete, Procedia Struct. Integr. 10 (2018) 155–162.
[72] Y. Chen, et al., Characterization of air-void systems in 3D printed cementitious materials using optical image scanning and X-ray computed tomography, Mater. Char. 173 (2021) 110948.
[73] H. Yue, et al., Investigation on applicability of spherical electric arc furnace slag as fine aggregate in superplasticizer-free 3D printed concrete, Construct. Build. Mater. 319 (2022) 126104.
[74] B. Nematollahi, et al., Effect of polypropylene fibre addition on properties of geopolymers made by 3D printing for digital construction, Materials 11 (12) (2018) 2352.
[75] S. Zou, et al., On rheology of mortar with recycled fine aggregate for 3D printing, Construct. Build. Mater. 311 (2021) 125312.
[76] Q. Deng, et al., Development and characteristic of 3D-printable mortar with waste glass powder, Buildings 13 (6) (2023) 1476.
[77] Y. Yin, et al., Effect of Hydroxypropyl methyl cellulose (HPMC) on rheology and printability of the first printed layer of cement activated slag-based 3D printing concrete, Construct. Build. Mater. 405 (2023) 133347.
[78] U. Kilic, et al., Effects of viscosity modifying admixture and nanoclay on fresh and rheo-viscoelastic properties and printability characteristics of cementitious composites, J. Build. Eng. 70 (2023) 106355.
[79] R. Jayathilakage, P. Rajeev, J. Sanjayan, Rheometry for concrete 3D printing: a review and an experimental comparison, Buildings 12 (8) (2022) 1190.
[80] T.T. Le, et al., Mix design and fresh properties for high-performance printing concrete, Mater. Struct. 45 (2012) 1221–1232.
[81] G. Bai, et al., 3D printing eco-friendly concrete containing under-utilised and waste solids as aggregates, Cement Concr. Compos. 120 (2021) 104037.
[82] A. Douba, S. Kawashima, Use of nanoclays and methylcellulose to tailor rheology for three-dimensional concrete printing, ACI Mater. J. 118 (6) (2021).
[83] M.T. Souza, et al., Role of chemical admixtures on 3D printed Portland cement: assessing rheology and buildability, Construct. Build. Mater. 314 (2022) 125666.
[84] Y. Chen, et al., The effect of viscosity-modifying admixture on the extrudability of limestone and calcined clay-based cementitious material for extrusion-based 3D concrete printing, Materials 12 (9) (2019) 1374.
[85] D.G. Soltan, V.C. Li, A self-reinforced cementitious composite for building-scale 3D printing, Cement Concr. Compos. 90 (2018) 1–13.
[86] G. Ma, L. Wang, A critical review of preparation design and workability measurement of concrete material for largescale 3D printing, Front. Struct. Civ. Eng. 12 (2018) 382–400.
[87] Y.W. Tay, et al., Processing and properties of construction materials for 3D printing, in: Materials Science Forum, Trans Tech Publ, 2016.
[88] V. Nerella, et al., Inline quantification of extrudability of cementitious materials for digital construction, Cement Concr. Compos. 95 (2019) 260–270.
[89] Z. Xu, et al., Effect of FA and GGBFS on compressive strength, rheology, and printing properties of cement-based 3D printing material, Construct. Build. Mater. 339 (2022) 127685.
[90] H. Varela, G. Barluenga, A. Perrot, Extrusion and structural build-up of 3D printing cement pastes with fly ash, nanoclays and VMAs, Cement Concr. Compos. 142 (2023) 105217.
[91] B. Panda, S.C. Paul, M.J. Tan, Anisotropic mechanical performance of 3D printed fiber reinforced sustainable construction material, Mater. Lett. 209 (2017) 146–149.
[92] S. Chaves Figueiredo, et al., Mechanical behavior of printed strain hardening cementitious composites, Materials 13 (10) (2020) 2253.
[93] A. Rahul, et al., 3D printable concrete: mixture design and test methods, Cement Concr. Compos. 97 (2019) 13–23.
[94] J. Xiao, et al., Large-scale 3D printing concrete technology: current status and future opportunities, Cement Concr. Compos. 122 (2021) 104115.
[95] Y. Zhao, et al., Effects of rheological properties and printing speed on molding accuracy of 3D printing basalt fiber cementitious materials, J. Mater. Res. Technol. 21 (2022) 3462–3475.
[96] S.C. Figueiredo, et al., An approach to develop printable strain hardening cementitious composites, Mater. Des. 169 (2019) 107651.
[97] Y. Weng, et al., Empirical models to predict rheological properties of fiber reinforced cementitious composites for 3D printing, Construct. Build. Mater. 189 (2018) 676–685.
[98] M.S. Choi, S.B. Park, S.-T. Kang, Effect of the mineral admixtures on pipe flow of pumped concrete, J. Adv. Concr. Technol. 13 (11) (2015) 489–499.
[99] Q. Wang, et al., Effect of fly ash on rheological properties of graphene oxide cement paste, Construct. Build. Mater. 138 (2017) 35–44.

[100] Y. Chen, et al., Improving printability of limestone-calcined clay-based cementitious materials by using viscosity-modifying admixture, Cement Concr. Res. 132 (2020) 106040.
[101] A. Kazemian, et al., Cementitious materials for construction-scale 3D printing: laboratory testing of fresh printing mixture, Construct. Build. Mater. 145 (2017) 639–647.
[102] B. Panda, et al., Improving the 3D printability of high volume fly ash mixtures via the use of nano attapulgite clay, Compos. B Eng. 165 (2019) 75–83.
[103] M. Chen, et al., Effect of tartaric acid on the printable, rheological and mechanical properties of 3D printing sulphoaluminate cement paste, Materials 11 (12) (2018) 2417.
[104] B. Panda, M.J. Tan, Experimental study on mix proportion and fresh properties of fly ash based geopolymer for 3D concrete printing, Ceram. Int. 44 (9) (2018) 10258–10265.
[105] N. Roussel, Rheological requirements for printable concretes, Cement Concr. Res. 112 (2018) 76–85.
[106] A. Perrot, D. Rangeard, 3D printing in concrete: techniques for extrusion/casting. 3D Printing of Concrete: State of the Art and Challenges of the Digital Construction Revolution, 2019, pp. 41–72.
[107] C.F. Ferraris, Measurement of the rheological properties of high performance concrete: state of the art report, Journal of research of the national institute of standards and technology 104 (5) (1999) 461.
[108] J. Zhang, et al., A review of the current progress and application of 3D printed concrete, Compos. Appl. Sci. Manuf. 125 (2019) 105533.
[109] J. Xiao, et al., Rheology of 3D printable concrete prepared by secondary mixing of ready-mix concrete, Cement Concr. Compos. 138 (2023) 104958.
[110] Y. Qian, S. Kawashima, Distinguishing dynamic and static yield stress of fresh cement mortars through thixotropy, Cement Concr. Compos. 86 (2018) 288–296.
[111] J. Kruger, S. Zeranka, G. van Zijl, An ab initio approach for thixotropy characterisation of (nanoparticle-infused) 3D printable concrete, Construct. Build. Mater. 224 (2019) 372–386.
[112] V. Saruhan, M. Keskinateş, B. Felekoğlu, A comprehensive review on fresh state rheological properties of extrusion mortars designed for 3D printing applications, Construct. Build. Mater. 337 (2022) 127629.
[113] M.H. Ali, A. Abilgaziyev, D. Adair, 4D printing: a critical review of current developments, and future prospects, Int. J. Adv. Des. Manuf. Technol. 105 (2019) 701–717.
[114] M.T. Souza, et al., 3D printed concrete for large-scale buildings: an overview of rheology, printing parameters, chemical admixtures, reinforcements, and economic and environmental prospects, J. Build. Eng. 32 (2020) 101833.
[115] R. Rafiee, P. Sharifi, Stochastic failure analysis of composite pipes subjected to random excitation, Construct. Build. Mater. 224 (2019) 950–961.
[116] A.U. Rehman, J.-H. Kim, 3D concrete printing: a systematic review of rheology, mix designs, mechanical, microstructural, and durability characteristics, Materials 14 (14) (2021) 3800.
[117] B. Panda, et al., The effect of material fresh properties and process parameters on buildability and interlayer adhesion of 3D printed concrete, Materials 12 (13) (2019) 2149.
[118] Y. Weng, et al., Design 3D printing cementitious materials via Fuller Thompson theory and Marson-Percy model, Construct. Build. Mater. 163 (2018) 600–610.
[119] M.P. Tinoco, et al., The use of rice husk particles to adjust the rheological properties of 3D printable cementitious composites through water sorption, Construct. Build. Mater. 365 (2023) 130046.
[120] H. Lee, et al., Evaluation of the mechanical properties of a 3D-printed mortar, Materials 12 (24) (2019) 4104.
[121] M. Chen, et al., Rheological parameters, thixotropy and creep of 3D-printed calcium sulfoaluminate cement composites modified by bentonite, Compos. B Eng. 186 (2020) 107821.
[122] M.A. Moeini, M. Hosseinpoor, A. Yahia, Effectiveness of the rheometric methods to evaluate the build-up of cementitious mortars used for 3D printing, Construct. Build. Mater. 257 (2020) 119551.
[123] S.A. Nair, et al., A critical examination of the influence of material characteristics and extruder geometry on 3D printing of cementitious binders, Cement Concr. Compos. 112 (2020) 103671.
[124] D. Marchon, et al., Hydration and rheology control of concrete for digital fabrication: potential admixtures and cement chemistry, Cement Concr. Res. 112 (2018) 96–110.
[125] W. Schmidt, et al., Effects of superplasticizer and viscosity-modifying agent on fresh concrete performance of SCC at varied ambient temperatures, in: Design, Production and Placement of Self-Consolidating Concrete: Proceedings of SCC2010, Montreal, Canada, September 26-29, 2010, Springer, 2010.
[126] K.-K. Yun, S.-Y. Choi, J.H. Yeon, Effects of admixtures on the rheological properties of high-performance wet-mix shotcrete mixtures, Construct. Build. Mater. 78 (2015) 194–202.
[127] A. Leemann, F. Winnefeld, The effect of viscosity modifying agents on mortar and concrete, Cement Concr. Compos. 29 (5) (2007) 341–349.
[128] S. Ahmad, A. Lawan, M. Al-Osta, Effect of sugar dosage on setting time, microstructure and strength of Type I and Type V Portland cements, Case Stud. Constr. Mater. 13 (2020) e00364.
[129] M.V. Tran, Y.T. Cu, C.V. Le, Rheology and shrinkage of concrete using polypropylene fiber for 3D concrete printing, J. Build. Eng. 44 (2021) 103400.
[130] V. Mechtcherine, V.N. Nerella, K. Kasten, Testing pumpability of concrete using sliding pipe rheometer, Construct. Build. Mater. 53 (2014) 312–323.
[131] M. Choi, et al., Metrology needs for predicting concrete pumpability, Adv. Mater. Sci. Eng. (2015) 2015.
[132] G. Rojo-López, et al., Rheology, durability, and mechanical performance of sustainable self-compacting concrete with metakaolin and limestone filler, Case Stud. Constr. Mater. 17 (2022) e01143.
[133] S. Oh, S. Choi, Effects of superabsorbent polymers (SAP) on the rheological behavior of cement mortars: a rheological study on performance requirements for 3D printable cementitious materials, Construct. Build. Mater. 392 (2023) 131856.
[134] J. Liu, K.H. Khayat, C. Shi, Effect of superabsorbent polymer characteristics on rheology of ultra-high performance concrete, Cement Concr. Compos. 112 (2020) 103636.
[135] E. Secrieru, et al., Rheological characterisation and prediction of pumpability of strain-hardening cement-based-composites (SHCC) with and without addition of superabsorbent polymers (SAP) at various temperatures, Construct. Build. Mater. 112 (2016) 581–594.
[136] X. Ma, et al., Effect of water absorption of SAP on the rheological properties of cement-based materials with ultra-low w/b ratio, Construct. Build. Mater. 195 (2019) 66–74.